The Innovation, Volume *2*

Supplemental Information

Subtle Side Chain Triggers Unexpected Two-Channel Charge Transport Property Enabling 80% Fill Factors and Efficient Thick-Film Organic Photovoltaics

Yonghai Li, Lu Yu, Liangliang Chen, Chenyu Han, Huanxiang Jiang, Zitong Liu, Nan Zheng, Jiuxing Wang, Mingliang Sun, Renqiang Yang, and Xichang Bao

Supporting Information

Subtle Side Chain Triggers Unexpected Two-Channel Charge Transport Property Enabling 80% Fill Factors and Efficient Thick-Film Organic Photovoltaics

Yonghai Li,*[a,c] Lu Yu,[a,b] Liangliang Chen,[d] Chenyu Han,[a] Huanxiang Jiang,[a] Zitong Liu,[d] Nan Zheng,*[e] Jiuxing Wang,[f] Mingliang Sun,[b] Renqiang Yang*[a,g] and Xichang Bao*[a,c]

[a] CAS Key Laboratory of Bio-based Materials, Qingdao Institute of Bioenergy and Bioprocess Technology, Chinese Academy of Sciences, Qingdao 266101, China.

[b] School of Material Science and Engineering, Ocean University of China, Qingdao 266100, China

[c] Functional Laboratory of Solar Energy, Shandong Energy Institute, Qingdao 266101, China

[d] Beijing National Laboratory for Molecular Sciences, CAS Key Laboratory of Organic Solids, Institute of Chemistry, Chinese Academy of Sciences, Beijing 100190, China

[e] State Key Laboratory of Luminescent Materials and Devices, South China University of Technology, Guangzhou 510640, China.

[f] School of Materials Science and Engineering, Qingdao University, Qingdao 266071, China

[g] Key Laboratory of Optoelectronic Chemical Materials and Devices (Ministry of Education), School of Chemical and Environmental Engineering, Jianghan University, Wuhan 430056, China

E-mail: liyh@qibebt.ac.cn (Y. L.); zhengn@scut.edu.cn (N. Z.); yangrq@qibebt.ac.cn (R. Y.); baoxc@ qibebt.ac.cn (X. B.)

Experimental Procedures

Materials and Characterization Techniques

Donor material PBDB-TF were purchased from Solarmer Materials Inc. The compound IDT was purchased from Derthon Co. All solvents and reagents were purchased from Alfa Aesar, Sigma-Aldrich, et al., which were utilized directly unless stated otherwise.

^{1}H NMR and ^{13}C NMR spectra were recorded on Bruker AVANCE III 600 MHz or Bruker AVANCE III 400 MHz spectrometer at 298 K. TGA measurement was performed using a SDT Q600 V20.9 Build 20 at a heating rate of 10 ^{o}C min^{-1} under a nitrogen atmosphere. The absorption spectra were recorded using a Hitachi U-4100 UV-Vis scanning spectrophotometer. Cyclic voltammetry (CV) measurements were performed on a CHI660D electrochemical workstation, equipped with a three-electrode cell consisting of a platinum working electrode, a saturated calomel electrode (SCE) as reference electrode and a platinum wire counter electrode. CV measurements were carried out in anhydrous acetonitrile containing 0.1 M *n*-Bu_4NPF_6 as a supporting electrolyte under an argon atmosphere at a scan rate of 100 mV s^{-1} assuming that the absolute energy level of Fc/Fc^{+} was -4.80 eV. Thin films were deposited from $CHCl_3$ solution onto the working electrodes. Grazing incidence wide-angle X-ray scattering (GIWAXS) patterns were acquired by detector Pilatus3R 1M, Dectris (X-ray Source: MetalJet-D2, Excillum). Transmission electron microscopy (TEM) images were obtained by using a HITACHI H-7650 electron microscope with an acceleration voltage of 100kV. Atomic force microscopy (AFM) images were obtained using Agilent 5400 scanning probe microscope in tapping mode with MikroMasch NSC-15 AFM tips. The X-ray crystallographic data were collected from Single crystal X-ray diffractometer (Synergy-R, Hybrid-CMOS 2D detector).

Device Fabrication and Evaluations

Photovoltaic devices were fabricated with a conventional device structure of ITO/PEDOT:PSS/PBDB-TF:IDIC-C*x*Ph/PDINO/Al. The patterned ITO glass (sheet resistance = 15 Ω/ square) was pre-cleaned in an ultrasonic bath of acetone and isopropyl alcohol and treated in an ultraviolet-ozone chamber (PREEN II-862) for 6 min. Then a thin layer (about 30 nm) of PEDOT:PSS was spin-coated onto the ITO glass at 4000 rpm and baked at 150 ^{o}C for 15 min. Solutions of PBDB-TF/ IDIC-C*x*Ph in chlorobenzene (18 mg/mL, total concentration) were stirred overnight and warmed to 50 ^{o}C for 30 mins before spin-coating on the PEDOT:PSS layer to form the active layer about 100±30 nm. The thickness of the active layer was measured using a Veeco Dektak 150 profilometer. Then PDINO solution (in CH_3OH, 1mg/mL) was spin-coating at 3000 rpm to form the electron transfer layer. Finally, Al (60 nm) metal electrode was thermal evaporated under about 4×10^{-4} Pa and the device area was 0.1 cm^2 defined by shadow mask.

The current density–voltage (*J–V*) characteristics were recorded with a Keithley 2400 source measurement under simulated 100 mW cm^{-2} irradiation from a SciSun-300 solar simulator. The *J–V* measurements were conducted without a correction window. The external quantum efficiencies (EQEs) were analysed EQE measurments through the Enlitech QE-R3011 quantum efficiency measurement system. The light intensity was calibrated with a standard single-crystal Si photovoltaic cell. The beam size is 5 cm × 5 cm. The voltage step and delay time were 10 mV and 3 ms, respectively. The scan started from −0.2 V to 1.4 V. The hole mobility and electron mobility were measured by space-charge-limited current (SCLC) method with a device

configuration of ITO/PEDOT:PSS/active layer/MoO_3/Al and ITO/ZnO/active layer/PFN/Al structure, respectively. The SCLC is described by the Mott–Gurney law:

$J = 9\varepsilon\mu V^2/(8L^3)$

where ε represents the dielectric constant of the metal, and μ is the carrier mobility, V is the voltage drop across the device and L is the thickness of the active layer.

The details for single crystals cultivation

The acceptor (IDIC-C4Ph, IDIC-C5Ph and IDIC-C6Ph) was dissolved in chloroform (~1mg/mL, 8 mg) and sealed in a small vial (volume: 15 mL) by aluminium-foil paper. Then several (4~6) pinholes were made on the foil paper by fine needle and put the small vial into a large-sized vial (volume: 50 mL), which contains 10 mL n-hexane. Finally, the large-sized vial was tightly sealed and put into a quiet and dark place at room temperature for 5~7 days to culture the single crystals.

The details for TA-SVA post-treatment

After spin-coating the active layer, or the neat donor or acceptor film onto ITO/glass substrates, the sample was put into a Petri dish (dia. 20 cm). Then 75 μL chlorobenzene (CB) was injected evenly from the sides. Given the high boiling point (132.2 °C) of CB and the low vapour pressure at room temperature, the Petri dish containing the samples was put onto a heating stage (80 °C) in glove box to accelerate the volatilization of chlorobenzene, and kept for 10 min to fully realize the solvent vapour annealing. During the SVA, we can observe the emergence of CB vapour which was coagulated in the cover of the Petri dish from about 2.5 min to about 8 min. Thus the SVA treatment in this study is aided by TA treatment (TA-SVA post-treatment).

The thermal annealing (TA) treatment

TA treatments were performed on a heating stage (80 °C) and kept for 10 min in the glove box.

The synthetic details of acceptors

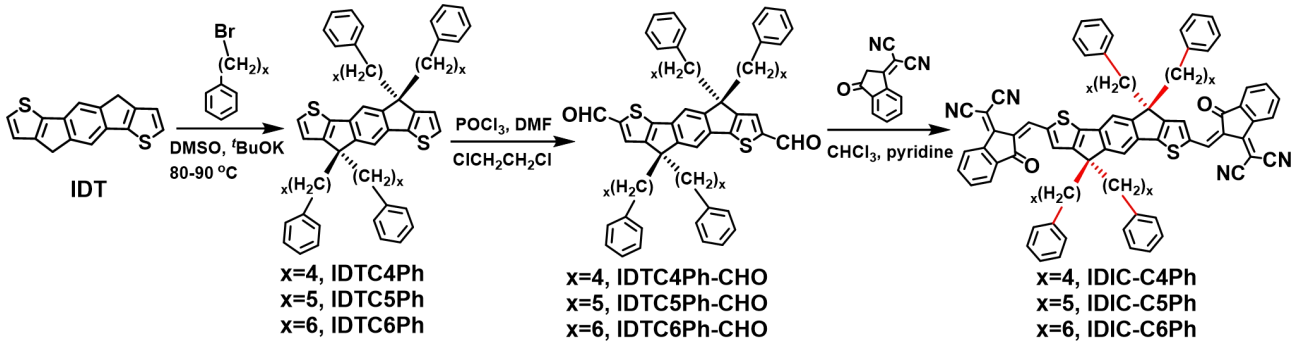

Scheme S1. The synthetic routes of IDIC-CxPh (x=4, 5, 6).

The IDIC-C4Ph was synthesized according to our previous report (*Adv. Mater*. 2019, 1807832).

Synthesis of IDTC5Ph: IDT (532.8 mg, 2.0 mmol) was dispersed in 15 mL dry DMSO and stirred under argon atmosphere. Then ^{t}BuOK (1.35 g, 12.0 mmol) was added in small portions. After then, the solution was heated at 80 ^{o}C for 1.0 hr. Subsequently, (5-bromopentyl)benzene (2.27 g, 1.85 mL, 10.0 mmol) was dropwise added into the solution and heated at 85-90 ^{o}C for another 5.0 hrs. When the solution cooled into room temperature, it was poured into ice water and extracted with dichloromethane (50 mL×3), dried with anhydrous Na_2SO_4, and removed the solvent by rotary evaporator. The crude product was subjected into silica gel column chromatography with petroleum ether: dichloromethane (4:1, v:v) as eluent to afford IDTC5Ph as pale solids (670 mg, yield: 40%). ^{1}H NMR (400 MHz, $CDCl_3$) δ 7.27 (m, 4H), 7.19 (m, 8H), 7.11 (m, 4H), 7.02 (m, 8H), 6.93 (d, J = 4.8 Hz, 2H), 2.39 (t, J = 7.7 Hz, 8H), 2.02 – 1.90 (m, 4H), 1.89 – 1.78 (m, 4H), 1.45 – 1.35 (m, 8H), 1.17 – 1.07 (m, 8H), 0.90 – 0.77 (m, 8H). ^{13}C NMR (101 MHz, $CDCl_3$) δ 155.08, 153.27, 142.84, 141.81, 135.80, 128.50, 128.27, 126.49, 125.61, 121.76, 113.26, 53.76, 39.20, 35.86, 31.19, 29.57, 24.02.

Synthesis of IDTC5Ph-CHO: Dry DMF (1.5 mL) dissolved into 10 mL 1, 2-dichloroethane was stirred at 0 ^{o}C under argon atmosphere. After dry $POCl_3$ (2 mL) was added dropwise, the solution was stirred at 0 ^{o}C for another 1.0 hr. Then IDTC5Ph (250 mg, 0.29 mmol) dissolved into 10 mL 1,2-dichloroethane was added dropwise. Then the solution was refluxed for 48 hrs under argon protection. When the solution cooled into room temperature, it was poured into ice water and stirred for 4.0 hrs and extracted with dichloromethane (30 mL×3), dried with anhydrous Na_2SO_4, and removed the solvent by rotary evaporator. The crude product was subjected into silica gel column chromatography with petroleum ether: dichloromethane (1:2, v:v) as eluent to afford IDTC5Ph-CHO as bright yellow solids (245 mg, yield: 93%). ^{1}H NMR (600 MHz, $CDCl_3$) δ 9.91 (s, 2H), 7.61 (s, 2H), 7.45 (s, 2H), 7.20 (m, 8H), 7.14 (m, 4H), 7.03 (m, 8H), 2.42 (m, 8H), 2.02 (m, 4H), 1.93 – 1.86 (m, 4H), 1.42 (m, 8H), 1.19 – 1.13 (m, 8H), 0.88 – 0.78 (m, 8H). ^{13}C NMR (151 MHz, $CDCl_3$) δ 183.12, 156.03, 155.20, 151.44, 145.88, 142.53, 136.66, 130.46, 128.45, 128.32, 125.75, 115.17, 54.35, 38.97, 35.84, 31.14, 29.45, 24.23.

Synthesis of IDIC-C5Ph: IDTC5Ph-CHO (230 mg, 0.25 mmol) and 2-(3-oxo-2,3-dihydro-1H-inden-1-ylidene)malononitrile (291 mg, 1.5 mmol) were dissolved into 30 mL $CHCl_3$ and stirred under argon atmosphere. Then pyridine (1.0 mL) was added dropwise. Then the solution was refluxed for 24 hrs. When the solution cooled into room temperature, most of the solvent was removed. The remaining solution was precipitated into CH_3OH, filtered and the residue was washed by 100 mL CH_3OH to remove most of the end-cap compound. Then the crude product was subjected into silica gel column chromatography with dichloromethane as eluent to afford IDIC-C5Ph as deep blue solids (185 mg, yield: 59%). ^{1}H NMR (600 MHz, $CDCl_3$) δ 8.97 (s, 2H), 8.72 (d, J = 7.3 Hz, 2H), 7.97 – 7.91 (m, 2H), 7.82 – 7.75 (m, 4H), 7.72 (s, 2H), 7.58 (s, 2H), 7.19 (m, 8H), 7.10 (m, 4H), 7.03 (m, 8H), 2.43 (m, 8H), 2.09 – 2.01 (m, 4H), 1.93 (m, 4H), 1.47 – 1.40 (m, 8H), 1.22 – 1.15 (m, 8H), 0.94 – 0.80 (m, 8H). ^{13}C NMR (151 MHz, $CDCl_3$) δ 188.42, 160.79, 160.07, 157.44, 156.61, 142.53, 141.32, 140.11, 138.55, 138.04, 137.76, 137.10, 135.29, 134.63, 128.46, 128.32, 125.72, 125.47, 123.91, 122.37, 116.13, 114.91, 114.85, 69.21, 54.40, 39.08, 35.88, 31.13, 29.51, 24.36. Elemental Analysis: C, 82.00; H, 5.92; N, 4.45; S, 5.09. found: C, 81.89; H, 5.91; N, 4.56; S, 5.37.

Synthesis of IDTC6Ph: IDT (500 mg, 1.88 mmol) was dispersed in 15 mL dry DMSO and stirred under argon atmosphere. Then ^{t}BuOK (1.26 g, 11.3 mmol) was added in small portions. After then, the solution was heated at 80 ^{o}C for 1.0 hr. Subsequently, (6-bromohexyl)benzene (3.60 g, 1.84 mL, 15.0 mmol) was dropwise added into the solution and heated at 85-90 ^{o}C for another 5.0 hrs. When the solution cooled into room

temperature, it was poured into ice water and extracted with dichloromethane (50 mL×3), dried with anhydrous Na_2SO_4, and removed the solvent by rotary evaporator. The crude product was subjected into silica gel column chromatography with petroleum ether: dichloromethane (4:1, v:v) as eluent to afford IDTC6Ph as pale solids (710 mg, yield: 42%). ^{1}H NMR (600 MHz, $CDCl_3$) δ 7.28 – 7.24 (m, 4H), 7.21 (m, 8H), 7.12 (m, 4H), 7.08 (m, 8H), 6.94 (d, *J* = 4.8 Hz, 2H), 2.50 – 2.44 (m, 8H), 1.99 – 1.91 (m, 4H), 1.86 – 1.79 (m, 4H), 1.46 – 1.41 (m, 8H), 1.13 (br, 16H), 0.87 – 0.81 (m, 8H). ^{13}C NMR (151 MHz, $CDCl_3$) δ 155.17, 153.36, 142.98, 141.77, 135.69, 128.50, 128.30, 126.39, 125.63, 121.86, 113.28, 53.74, 39.21, 36.01, 31.53, 29.94, 29.09, 24.22.

Synthesis of IDTC6Ph-CHO: Dry DMF (1.5 mL) dissolved into 10 mL 1, 2-dichloroethane was stirred at 0 ^{o}C under argon atmosphere. After dry $POCl_3$ (2 mL) was added dropwise, the solution was stirred at 0 ^{o}C for another 1.0 hr. Then IDTC6Ph (250 mg, 0.27 mmol) dissolved into 10 mL 1,2-dichloroethane was added dropwise. Then the solution was refluxed for 48 hrs under argon protection. When the solution cooled into room temperature, it was poured into ice water and stirred for 4.0 hrs and extracted with dichloromethane (30 mL×3), dried with anhydrous Na_2SO_4, and removed the solvent by rotary evaporator. The crude product was subjected into silica gel column chromatography with petroleum ether: dichloromethane (1:2, v:v) as eluent to afford IDTC6Ph-CHO as bright yellow solids (215 mg, yield: 83%). ^{1}H NMR (600 MHz, $CDCl_3$) δ 9.91 (s, 2H), 7.62 (s, 2H), 7.45 (s, 2H), 7.22 (m, 8H), 7.14 (m, 4H), 7.09 (m, 8H), 2.53 – 2.47 (m, 8H), 2.02 (m, 4H), 1.88 (m, 4H), 1.46 (m, 8H), 1.15 (br, 16H), 0.83 (m, 8H). ^{13}C NMR (151 MHz, $CDCl_3$) δ 183.13, 156.12, 155.29, 151.47, 145.81, 142.76, 136.57, 130.52, 128.45, 128.35, 125.74, 115.20, 54.33, 38.96, 35.96, 31.45, 29.85, 29.02, 24.37.

Synthesis of IDIC-C6Ph: IDTC6Ph-CHO (205 mg, 0.21 mmol) and 2-(3-oxo-2,3-dihydro-1H-inden-1-ylidene)malononitrile (248 mg, 1.2 mmol) were dissolved into 30 mL $CHCl_3$ and stirred under argon atmosphere. Then pyridine (1.0 mL) was added dropwise. After then , the solution was refluxed for 24 hrs. When the solution cooled into room temperature, most of the solvent was removed. The remaining solution was precipitated into CH_3OH, filtered and the residue was washed by 100 mL CH_3OH to remove most of the end-cap compound. Then the crude product was subjected into silica gel column chromatography with dichloromethane as eluent to afford IDIC-C6Ph as deep blue solids (220 mg, yield: 80%). ^{1}H NMR (600 MHz, $CDCl_3$) δ 8.97 (s, 2H), 8.71 (d, *J* = 7.5 Hz, 2H), 7.98 – 7.93 (m, 2H), 7.82 – 7.74 (m, 4H), 7.72 (s, 2H), 7.58 (s, 2H), 7.20 (m, 8H), 7.10 (m, 12H), 2.52 – 2.47 (m, 8H), 2.08 – 2.00 (m, 4H), 1.95 – 1.88 (m, 4H), 1.50 – 1.44 (m, 8H), 1.17 (s, 16H), 0.94 – 0.79 (m, 8H). ^{13}C NMR (151 MHz, $CDCl_3$) δ 188.45, 160.80, 160.16, 157.53, 156.70, 142.79, 141.30, 140.11, 138.58, 137.99, 137.88, 137.09, 135.28, 134.62, 128.46, 128.32, 125.68, 125.46, 123.90, 122.30, 116.17, 114.93, 114.86, 69.15, 54.39, 39.06, 35.97, 31.48, 29.86, 29.05, 24.47. Elemental Analysis: C, 82.16; H, 6.28; N, 4.26; S, 4.87. found: C, 82.03; H, 6.25; N, 4.30; S, 4.99.

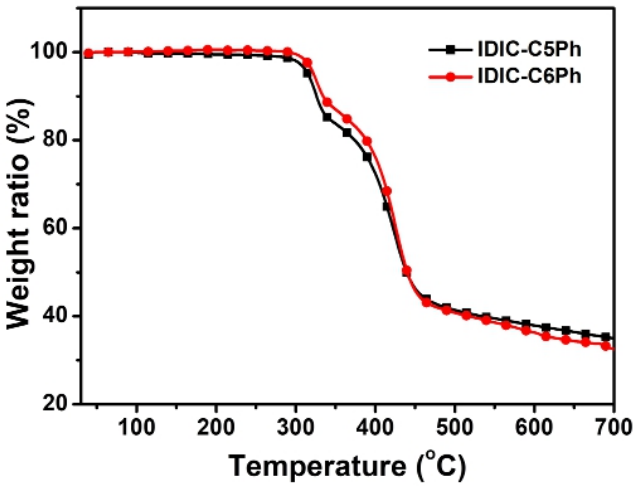

Figure. S1 TGA curves with a heating rate of 10 °C/min in N_2 atmosphere.

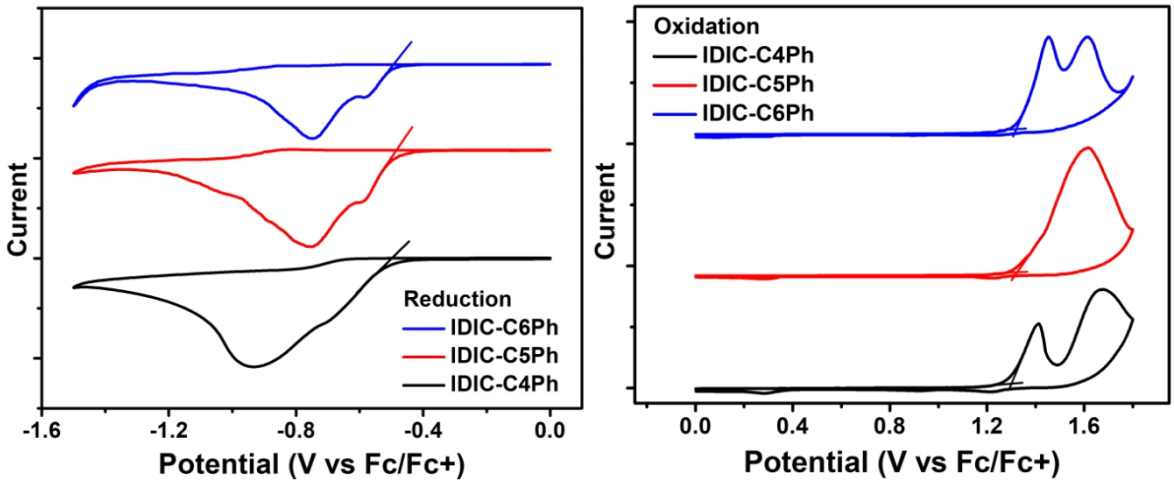

Figure S2. The cyclic voltammogram curves of IDIC-CxPh (x=4, 5, 6) on glassy carbon electrodes in 0.1 M Bu_4NPF_6-CH_3CN at a scan rate of 100 mV s^{-1}.

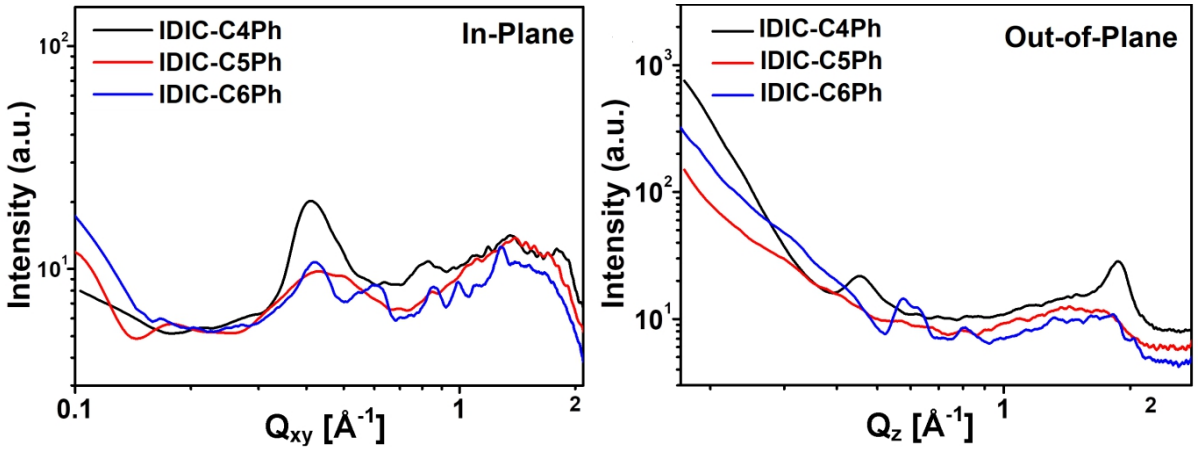

Figure S3. The line profiles of GIWAXS of IDIC-CxPh (x=4, 5, 6) films.

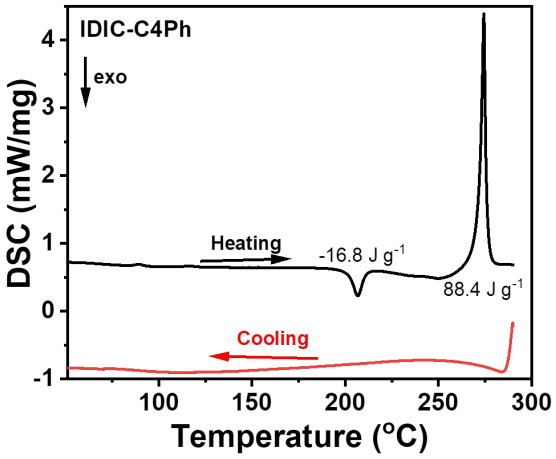

Figure S4. The DSC curves of IDIC-C4Ph powder with a heating rate of 10 °C/min in N_2 atmosphere.

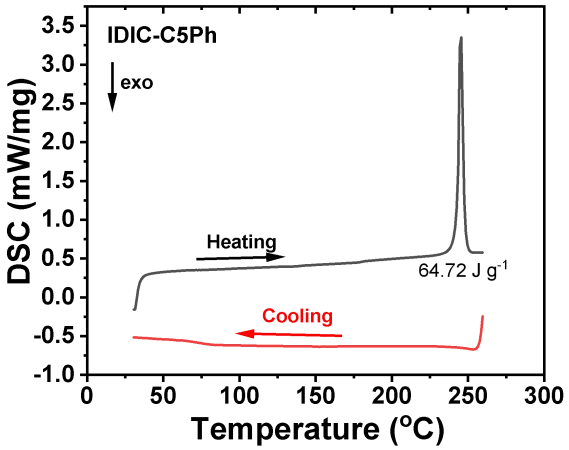

Figure S5. The DSC curves of IDIC-C5Ph powder with a heating rate of 10 °C/min in N_2 atmosphere.

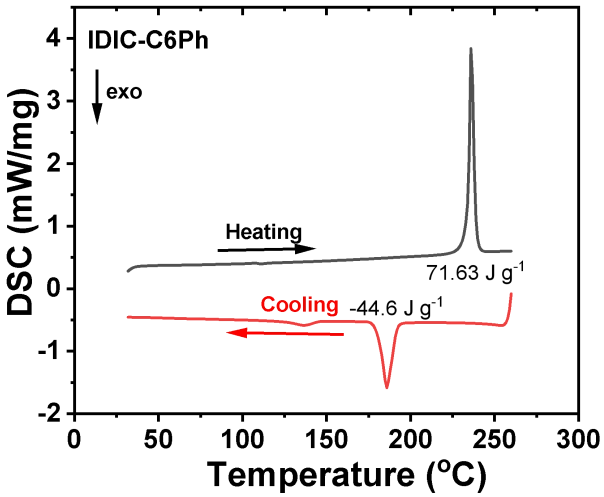

Figure S6. The DSC curves of IDIC-C6Ph powder with a heating rate of 10 °C/min in N_2 atmosphere.

Table S1. Crystal data and structure refinement for IDIC-C4Ph

CCDC number	1947277	
Identification code	IDIC-C4Ph	
Empirical formula	$C_{82}H_{66}N_4O_2S_2$	
Formula weight	1203.50	
Temperature	293(2) K	
Wavelength	1.54184 Å	
Crystal system	Monoclinic	
Space group	P 1 21/n 1	
Unit cell dimensions	a = 16.1333(4) Å	a= 90°.
	b = 21.4697(5) Å	b= 112.268(3)°.
	c = 20.8049(4) Å	g = 90°.
Volume	6668.9(3) $Å^3$	
Z	4	
Density (calculated)[a]	1.199 g cm^{-3}	
Absorption coefficient	1.119 mm^{-1}	
F(000)	2536	
Crystal size	0.2 x 0.15 x 0.1 mm^3	
Theta range for data collection	2.980 to 75.447°.	
Index ranges	-20<=h<=19, -25<=k<=26, -22<=l<=26	
Reflections collected	46993	
Independent reflections	13202 [R(int) = 0.0539]	
Completeness to theta = 67.684°	99.8 %	
Absorption correction	Semi-empirical from equivalents	
Max. and min. transmission	1.00000 and 0.58177	
Refinement method	Full-matrix least-squares on F^2	
Data / restraints / parameters	13202 / 790 / 1001	
Goodness-of-fit on F^2	1.427	
Final R indices [I>2sigma(I)]	R1 = 0.1109, wR2 = 0.3353	
R indices (all data)	R1 = 0.1381, wR2 = 0.3665	
Extinction coefficient	n/a	
Largest diff. peak and hole	1.328 and -0.498 e.$Å^{-3}$	

[a] The densities of the single crystals are automatically calculated from the SHELXL software based on the cell volume, Z value and molecular formula parameters.

Table S2. Crystal data and structure refinement for IDIC-C5Ph

CCDC number	1947278	
Identification code	IDIC-C5Ph	
Empirical formula	$C_{86}H_{74}N_4O_2S_2$	
Formula weight	1259.68	
Temperature	293(2) K	
Wavelength	1.54178 Å	
Crystal system	Triclinic	
Space group	P -1	
Unit cell dimensions	a = 15.08430(10) Å	a= 102.8640(10)°.
	b = 15.2016(2) Å	b= 95.0000(10)°.
	c = 16.6580(2) Å	g = 98.3670(10)°.
Volume	3655.85(7) $Å^3$	
Z	2	
Density (calculated) [a]	1.253 g cm-3	
Absorption coefficient	2.070 mm^{-1}	
F(000)	1448	
Crystal size	0.35 x 0.2 x 0.15 mm^3	
Theta range for data collection	2.742 to 75.355°.	
Index ranges	-18<=h<=18, -18<=k<=18, -20<=l<=11	
Reflections collected	31563	
Independent reflections	13149 [R(int) = 0.0195]	
Completeness to theta = 67.684°	93.2 %	
Absorption correction	Semi-empirical from equivalents	
Max. and min. transmission	1.000 and 0.7273	
Refinement method	Full-matrix least-squares on F^2	
Data / restraints / parameters	13149 / 108 / 920	
Goodness-of-fit on F^2	1.086	
Final R indices [I>2sigma(I)]	R1 = 0.0521, wR2 = 0.1342	
R indices (all data)	R1 = 0.0592, wR2 = 0.1516	
Extinction coefficient	n/a	
Largest diff. peak and hole	1.132 and -0.613 e.$Å^{-3}$	

[a] The densities of the single crystals are automatically calculated from the SHELXL software based on the cell volume, Z value and molecular formula parameters.

Table S3. Crystal data and structure refinement for IDIC-C6Ph

CCDC number	1947279	
Identification code	IDIC-C6Ph	
Empirical formula	$C_{90}H_{82}N_4O_2S_2$	
Formula weight	1315.79	
Temperature	293(2) K	
Wavelength	1.54178 Å	
Crystal system	Triclinic	
Space group	P -1	
Unit cell dimensions	a = 14.9275(3) Å	a= 82.8460(10)°.
	b = 15.8487(2) Å	b= 89.0300(10)°.
	c = 35.0092(5) Å	g = 76.3500(10)°.
Volume	7985.3(2) $Å^3$	
Z	4	
Density (calculated) [a]	1.194 g cm-3	
Absorption coefficient	1.913 mm^{-1}	
F(000)	3024	
Crystal size	0.6 x 0.35 x 0.07 mm^3	
Theta range for data collection	2.544 to 75.677°.	
Index ranges	-18<=h<=18, -19<=k<=19, -43<=l<=43	
Reflections collected	31663	
Independent reflections	31663 [R(int) = 0.052]	
Completeness to theta = 67.684°	99.8 %	
Absorption correction	Semi-empirical from equivalents	
Max. and min. transmission	1.0000 and 0.81573	
Refinement method	Full-matrix least-squares on F^2	
Data / restraints / parameters	31663 / 124 / 1875	
Goodness-of-fit on F^2	1.037	
Final R indices [I>2sigma(I)]	R1 = 0.0896, wR2 = 0.2637	
R indices (all data)	R1 = 0.1046, wR2 = 0.2785	
Extinction coefficient	n/a	
Largest diff. peak and hole	1.379 and -0.840 e.$Å^{-3}$	

[a] The densities of the single crystals are automatically calculated from the SHELXL software based on the cell volume, Z value and molecular formula parameters.

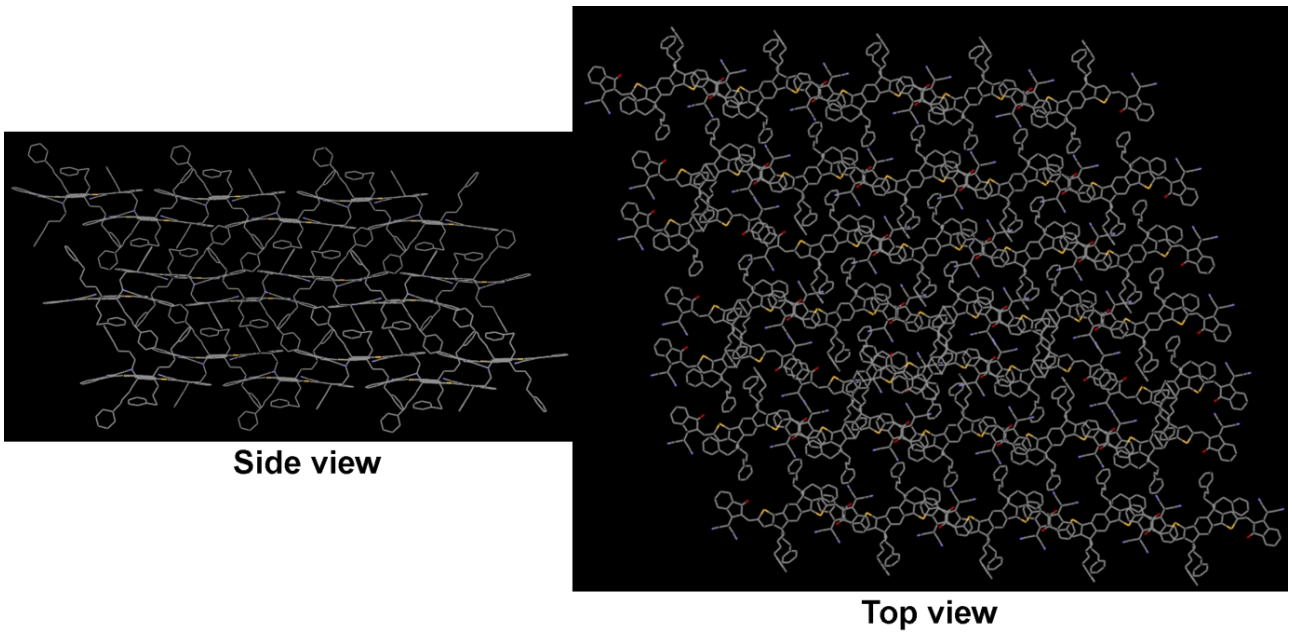

Figure S7. The molecular assembly in IDIC-C4Ph single crystal (H atoms are hidden).

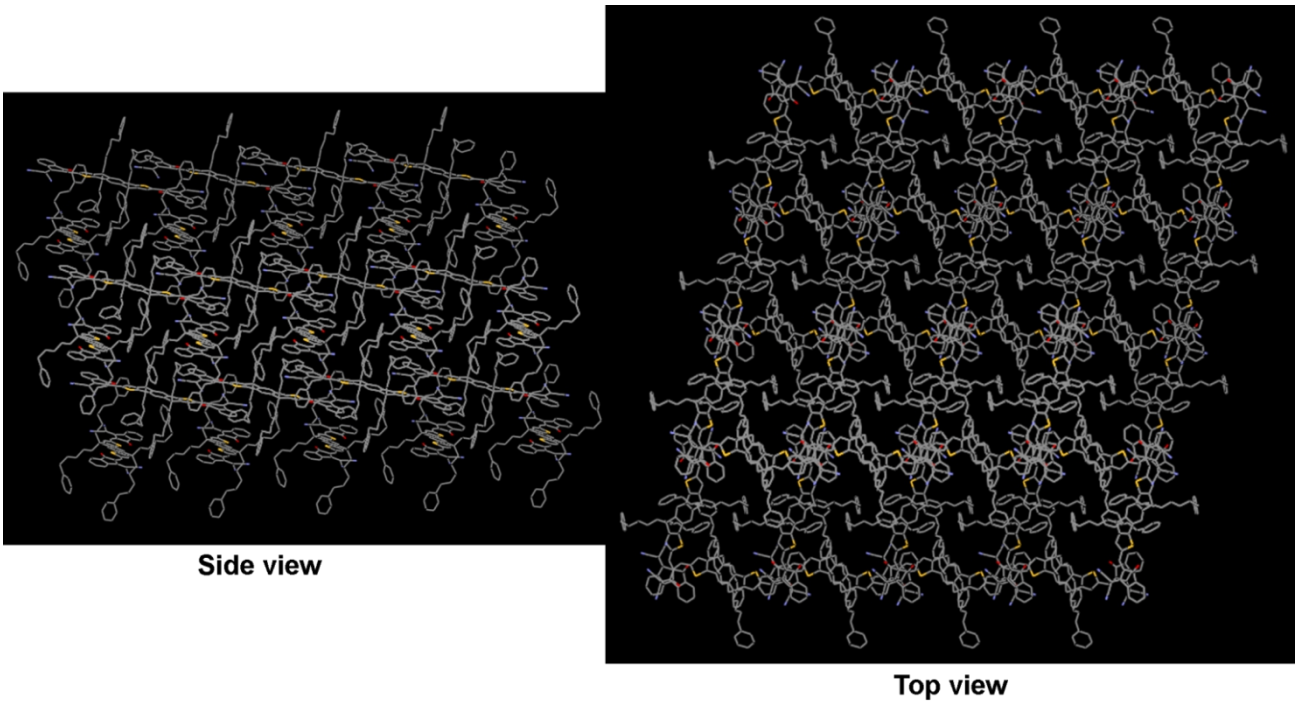

Figure S8. The molecular assembly in IDIC-C5Ph single crystal (H atoms are hidden; top view).

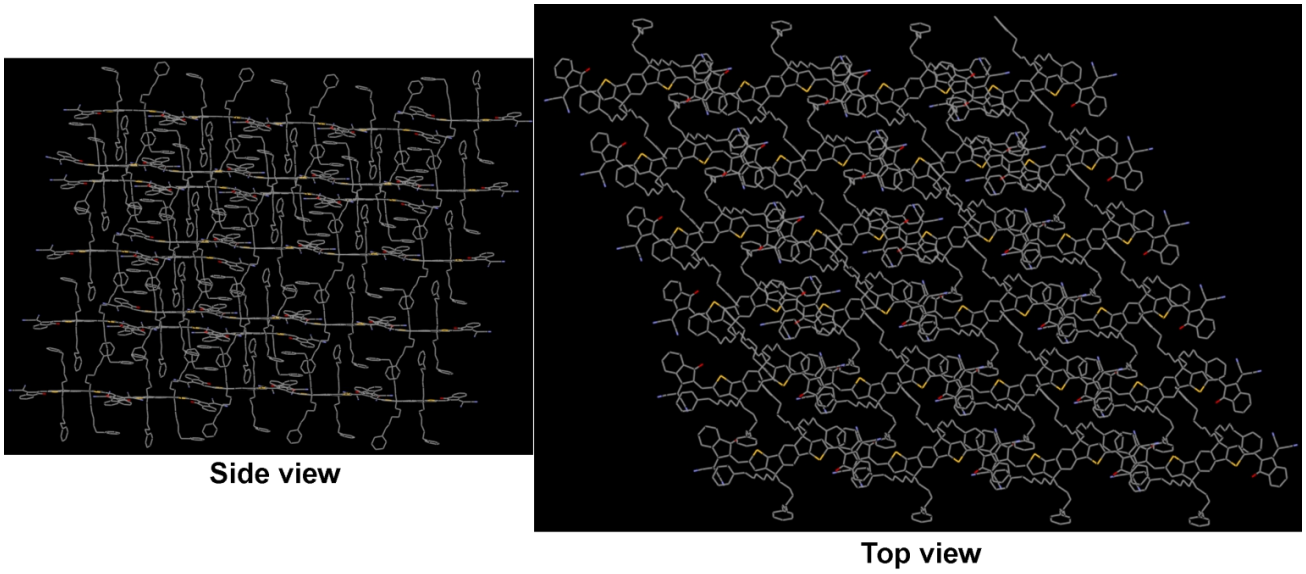

Figure S9. The molecular assembly in IDIC-C6Ph single crystal (H atoms are hidden).

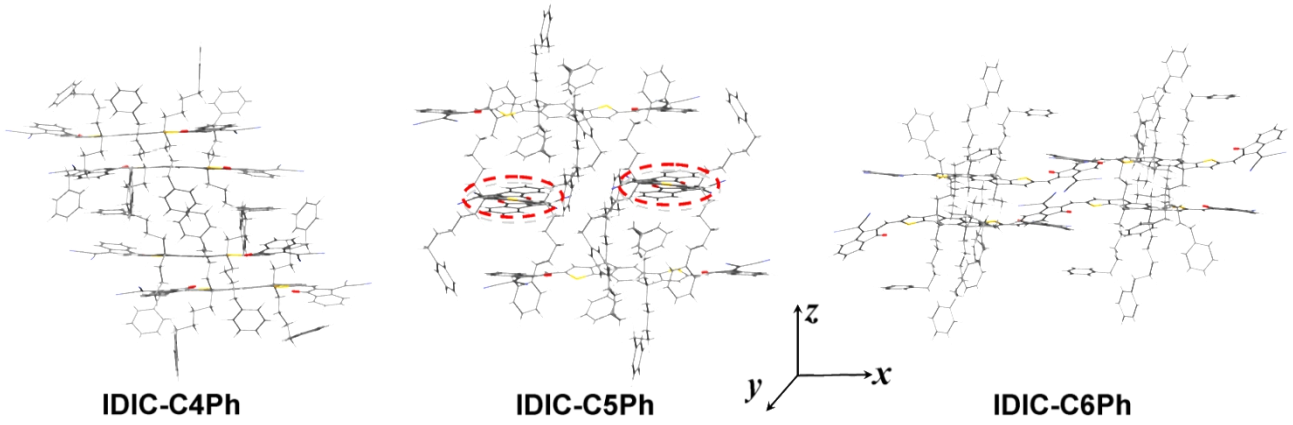

Figure S10. The molecular conformations and stacking of IDIC-CxPh (x=4, 5 and 6) based on DFT calculations with B3LYP-D3/def2-SVP algorithm.

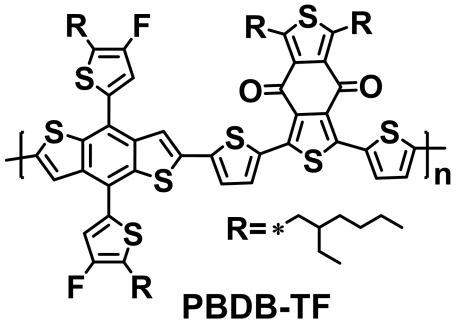

Figure S11. The chemical structure of polymer donor PBDB-TF used in this work.

Table S4. The photovoltaic parameters of as-cast OSCs with different donor/acceptor weight ratios under the illumination of AM 1.5G, 100 mW cm^{-2}

Acceptor	*Donor/acceptor*	V_{OC}	J_{SC}	FF	PCE
	w/w	(V)	(mA cm^{-2})	(%)	(%)[a]
IDIC-C4Ph	1:0.8	0.950	17.24	75.72	12.40 (12.14)
	1:1	0.952	18.06	76.77	13.20 (13.00)
	1:1.5	0.954	17.80	74.37	12.63 (12.32)
IDIC-C5Ph	1:0.8	0.956	17.69	69.33	11.72 (11.48)
	1:1	0.961	18.25	71.37	12.52 (12.24)
	1:1.5	0.963	18.02	70.11	12.17 (11.95)
IDIC-C6Ph	1:0.8	0.940	15.12	62.81	8.93 (8.77)
	1:1	0.949	16.03	66.68	10.14 (9.87)
	1:1.5	0.956	15.41	62.30	9.18 (9.00)

[a] The PCEs in brackets represent the average values based on at least 10 devices.

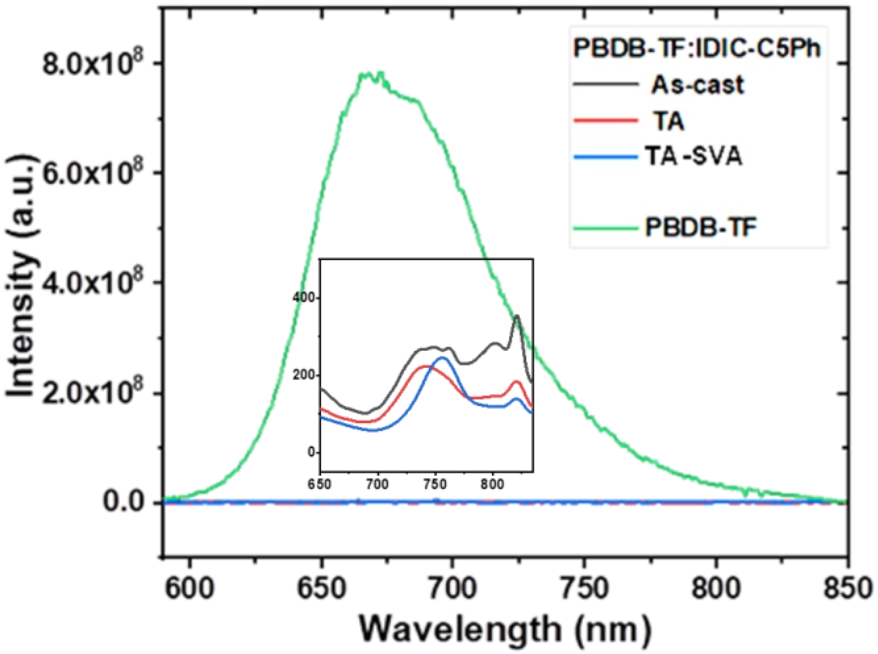

Figure S12. The PL spectra of neat PBDB-TF, BHJ blends under different conditions (excited at 580 nm). The inset is the enlarged PL spectra of blends.

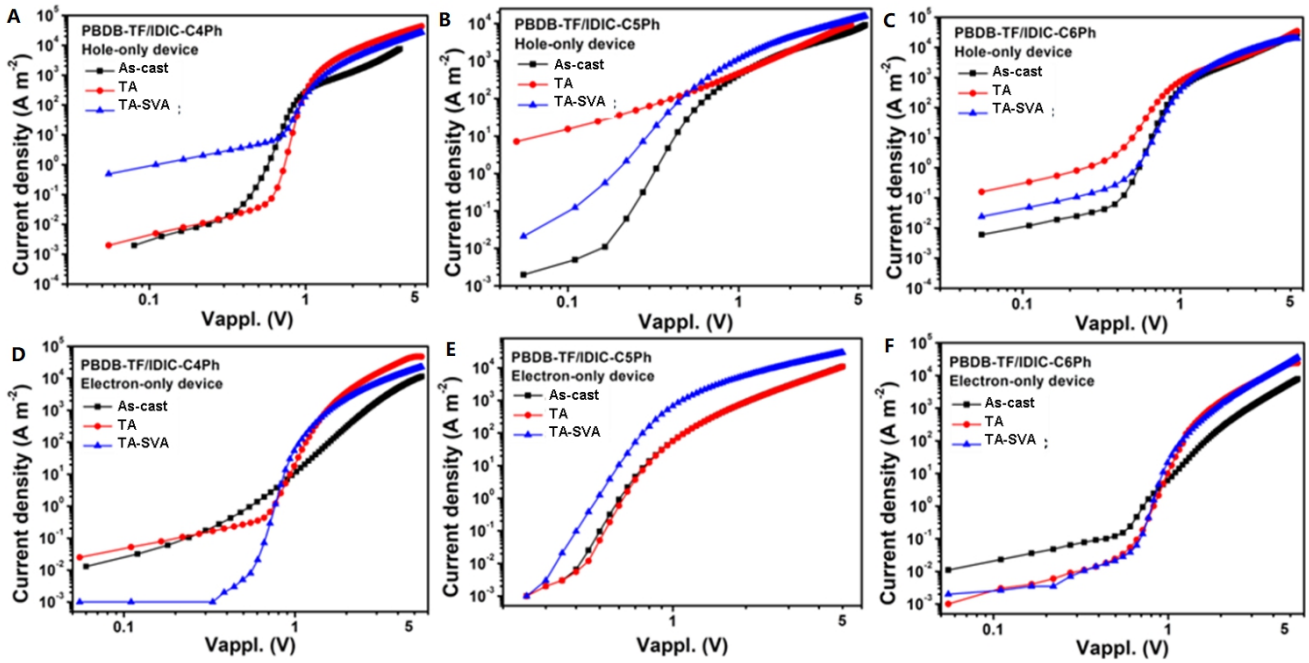

Figure S13. (A-C) The hole mobility and (D-F) electron mobility of OSCs with BHJsunder different conditions.

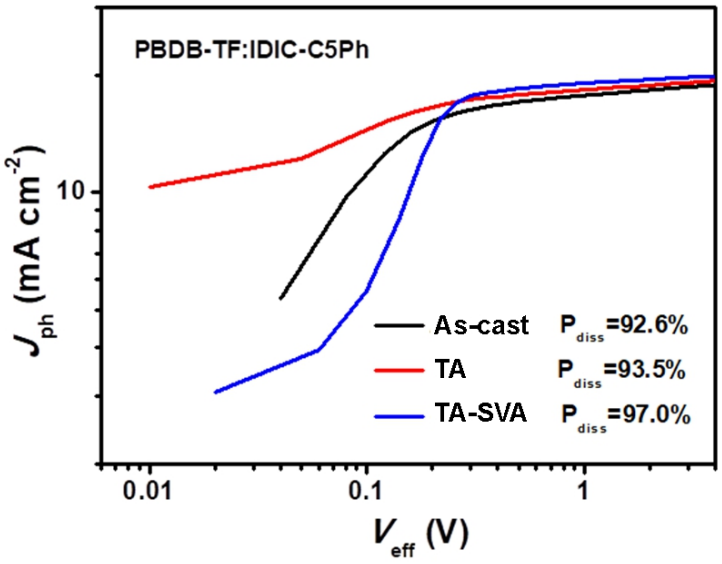

Figure S14. Photocurrent density (J_{ph}) plotted with respect to the effective bias (V_{eff}) for PBDB-TF:IDIC-C5Ph devices under different treatments.

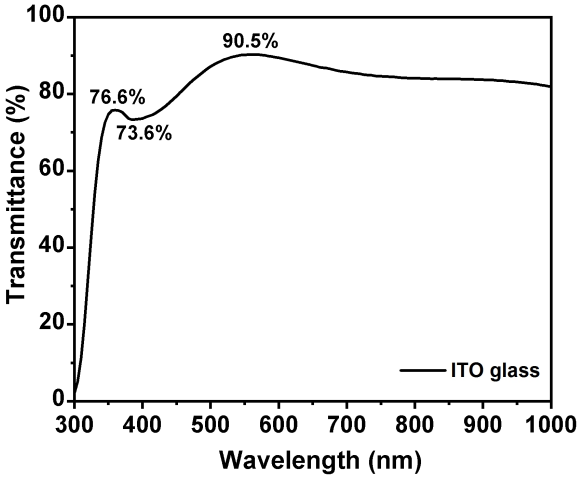

Figure S15. The transmittance curve of ITO glass.

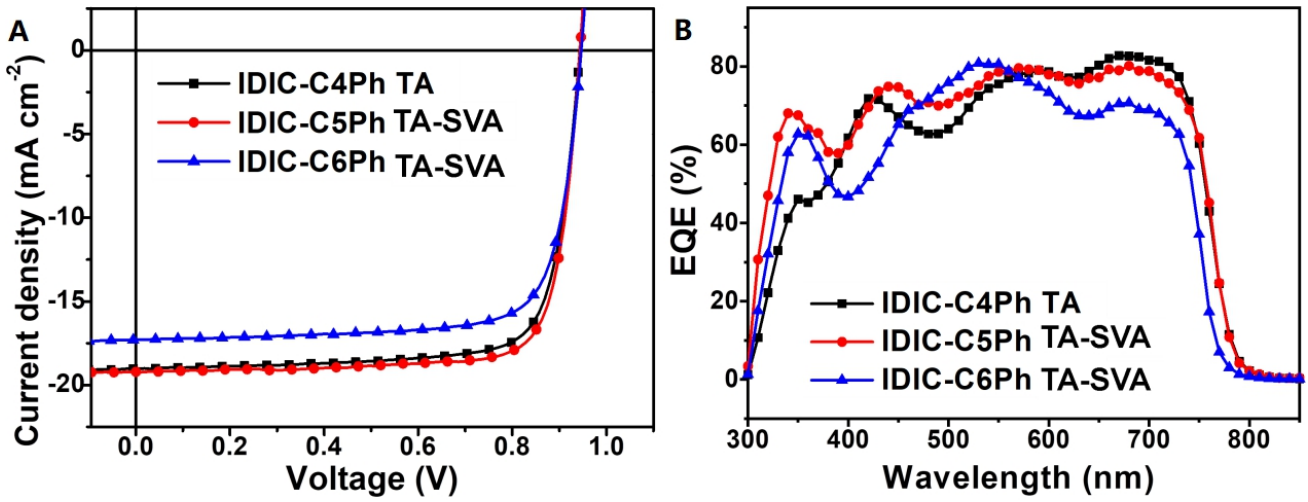

Figure S16. (A) The *J-V* curves of three optimized OSCs and (B) corresponding EQE curves.

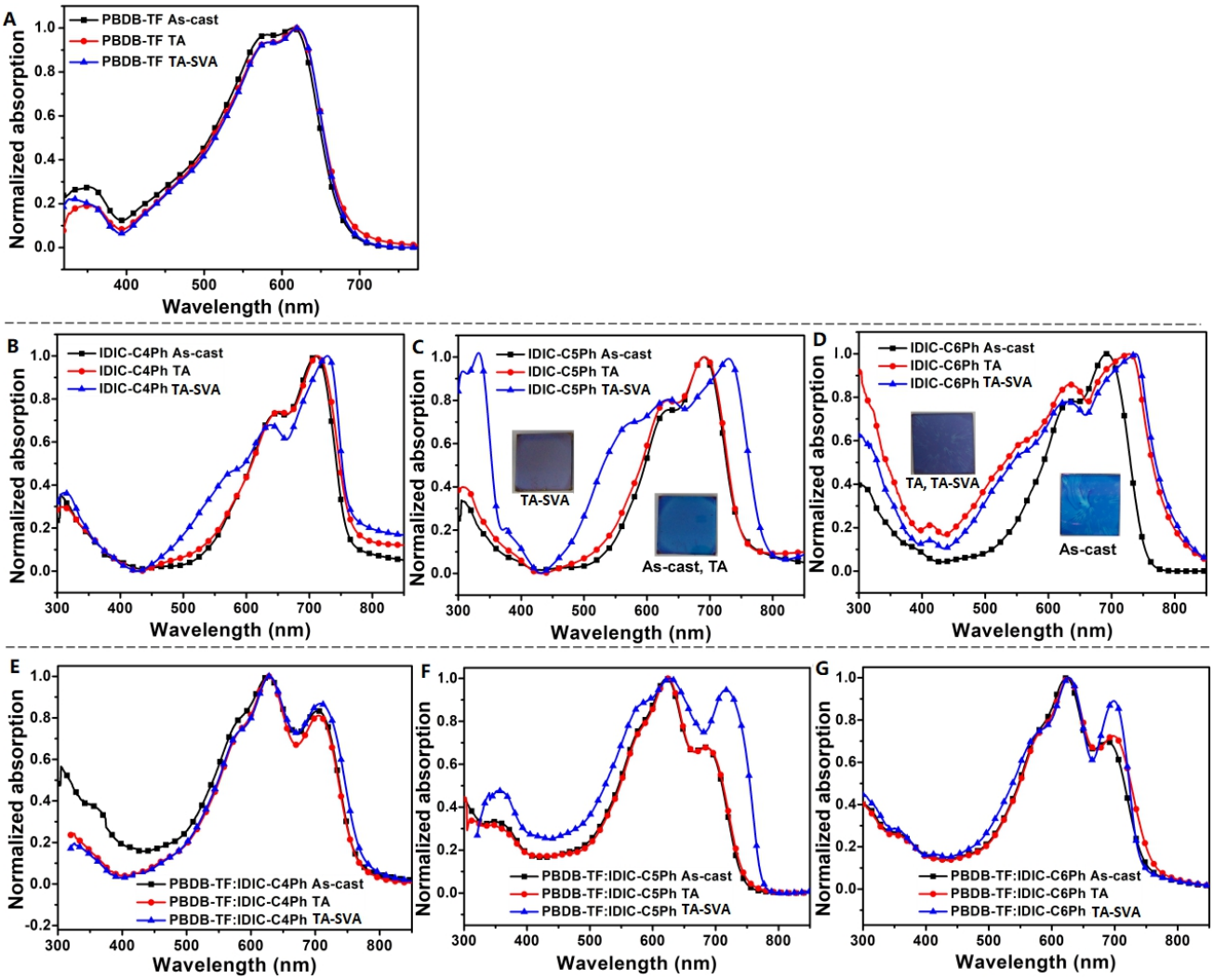

Figure S17. The absorption spectra of polymer PBDB-TF, three neat acceptors and respective blend films under different post-treatments.

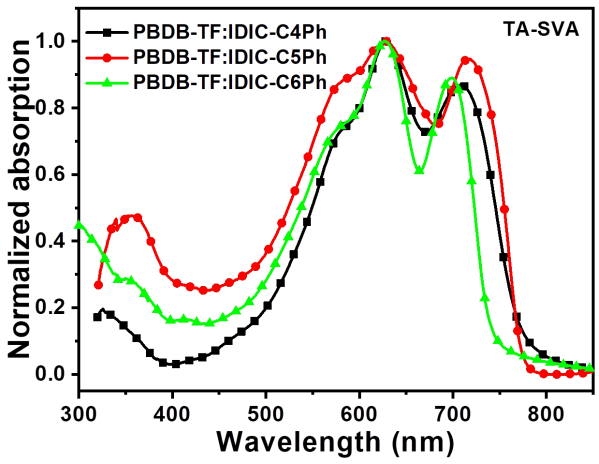

Figure S18. The absorption spectra of three BHJ blends under TA-SVA treatments.

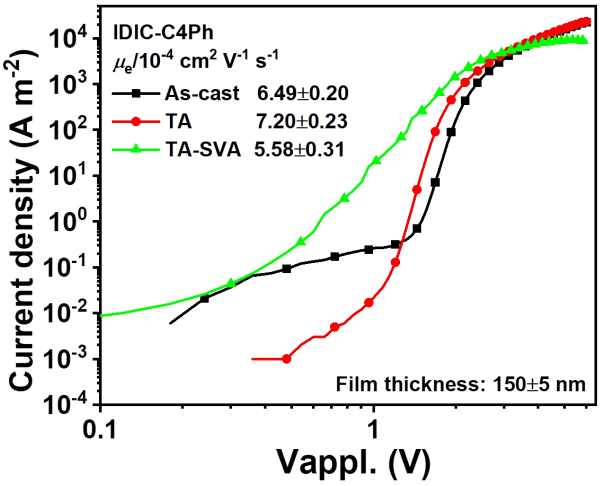

Figure S19. The SCLC curves and electron mobilities of pure acceptor IDIC-C4Ph under different treatments.

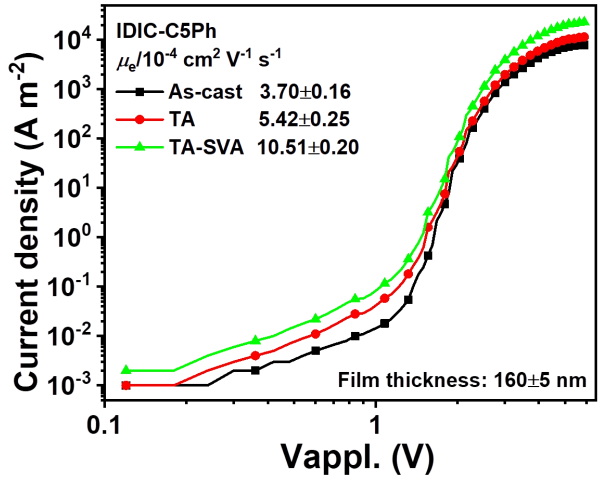

Figure S20. The SCLC curves and electron mobilities of pure acceptor IDIC-C5Ph under different treatments.

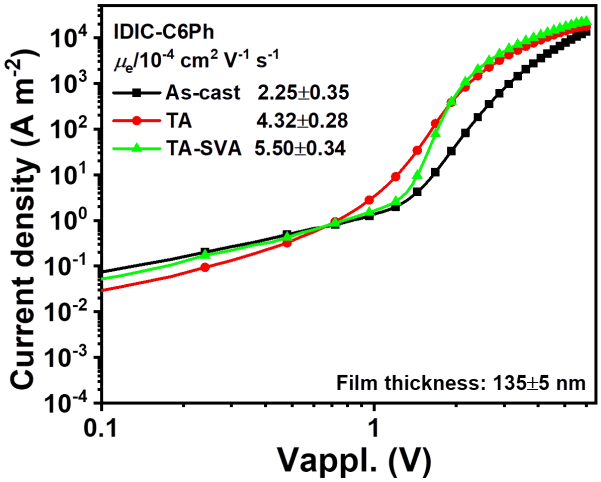

Figure S21. The SCLC curves and electron mobilities of pure acceptor IDIC-C6Ph under different treatments.

Table S5. The q locations and π-π-stacking distances in OOP direction of GIWAXS studies

Blend		q (Å^{-1})	$d_{spacing}$π-π (Å)
PBDB-TF:	As-cast	1.78	3.53
	TA	1.83	3.44
IDIC-C4Ph	TA-SVA	1.78	3.53
PBDB-TF:	As-cast	1.76	3.58
	TA	1.76	3.58
IDIC-C5Ph	TA-SVA	1.88	3.34
PBDB-TF:	As-cast	1.76	3.58
	TA	1.80	3.48
IDIC-C6Ph	TA-SVA	1.80	3.48

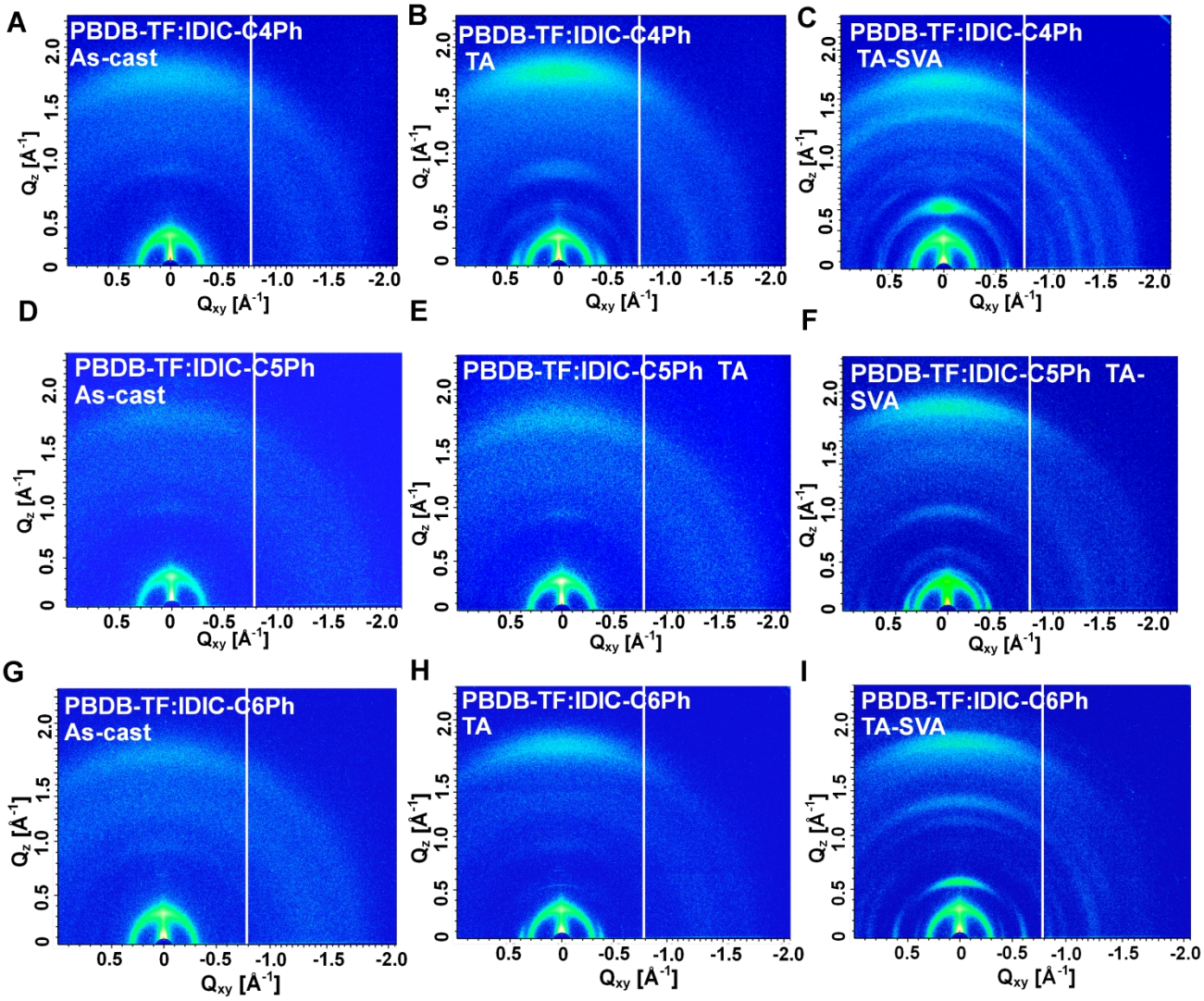

Figure S22. The 2D-GIWAXS images of PBDB-TF:IDIC-C4Ph (A-C), PBDB-TF:IDIC-C5Ph (D-F) and PBDB-TF:IDIC-C6Ph (G-I) under different treatments.

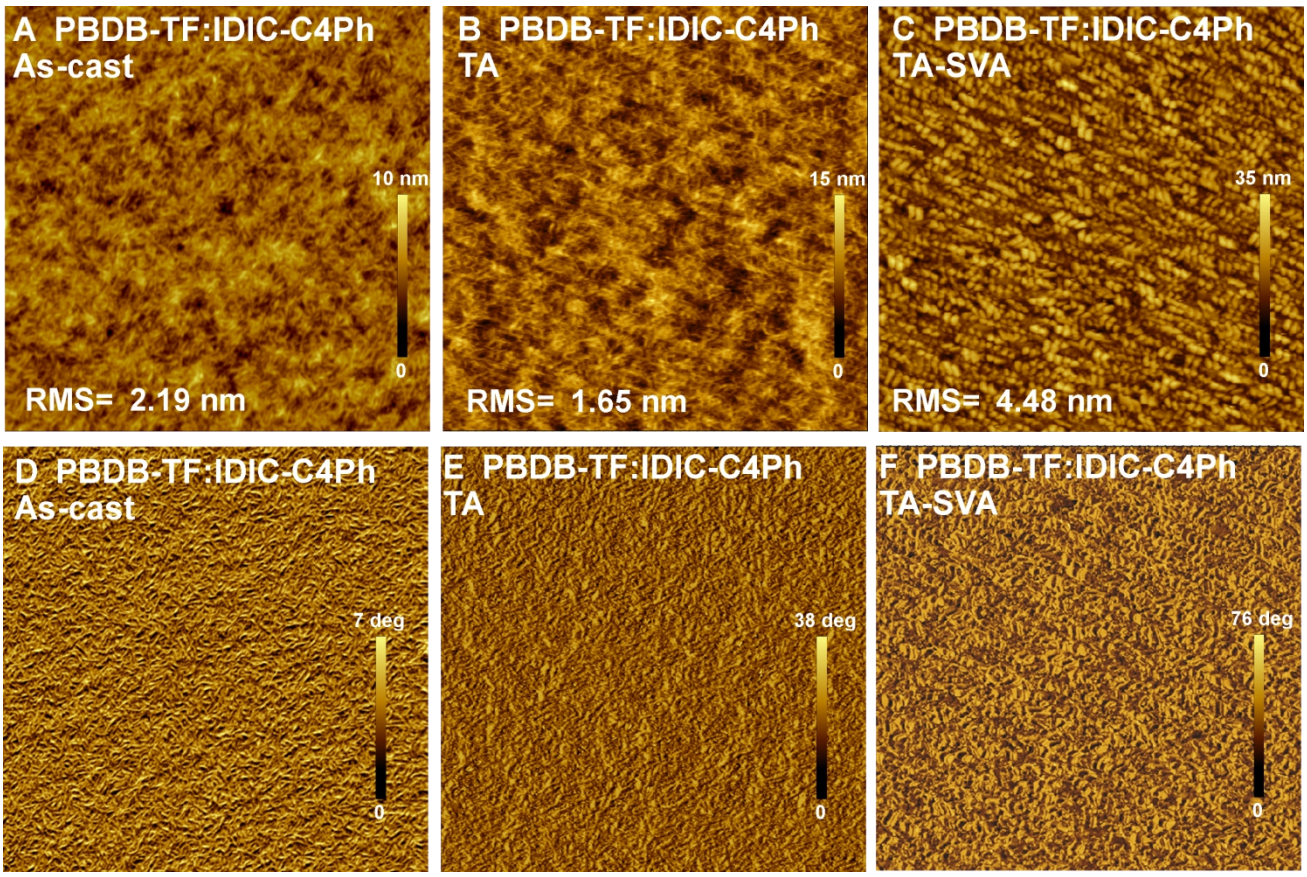

Figure S23. (A-C) The AFM and (D-F) phase images of PBDB-TF:IDIC-C4Ph under different treatments.

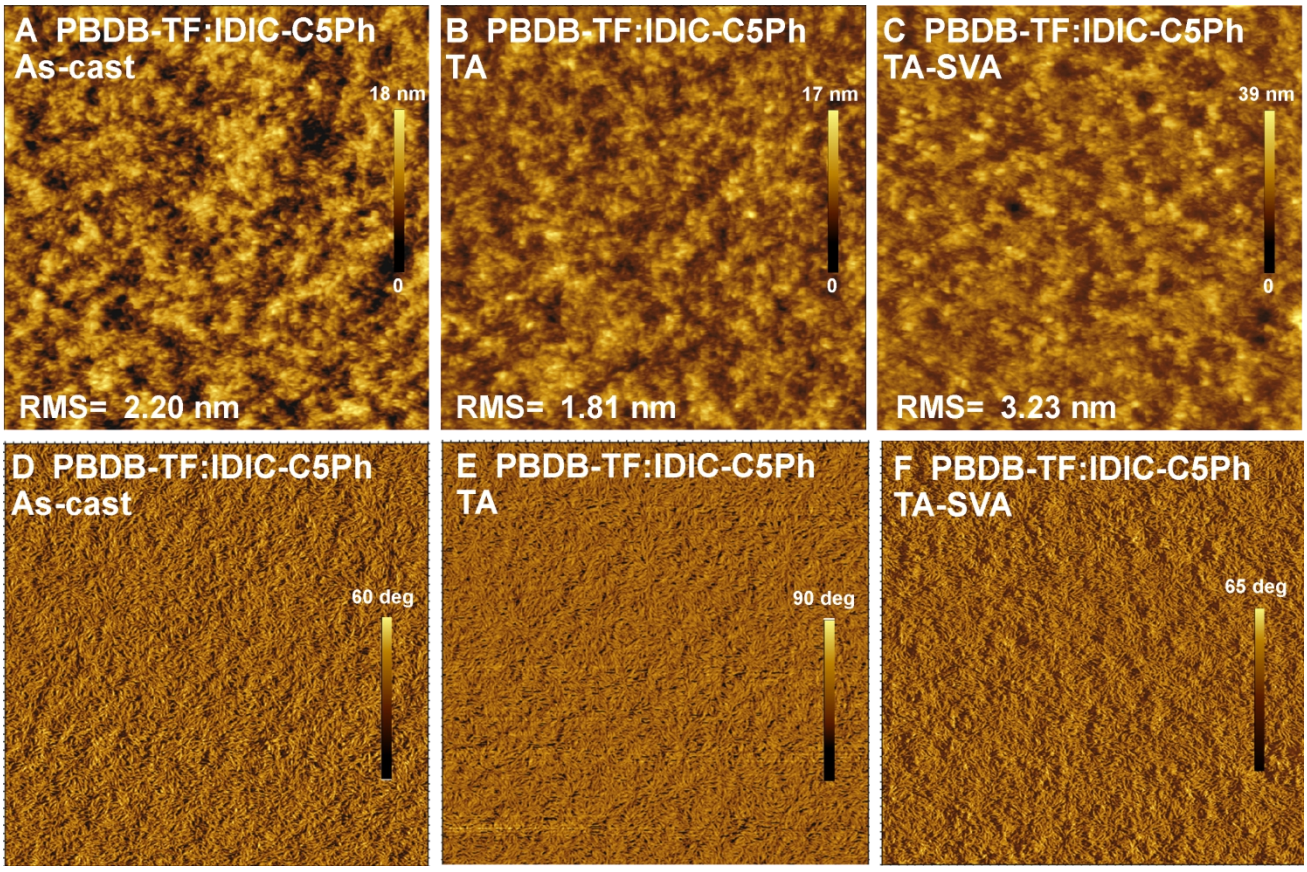

Figure S24. (A-C) The AFM and (D-F) phase images of PBDB-TF:IDIC-C5Ph under different treatments.

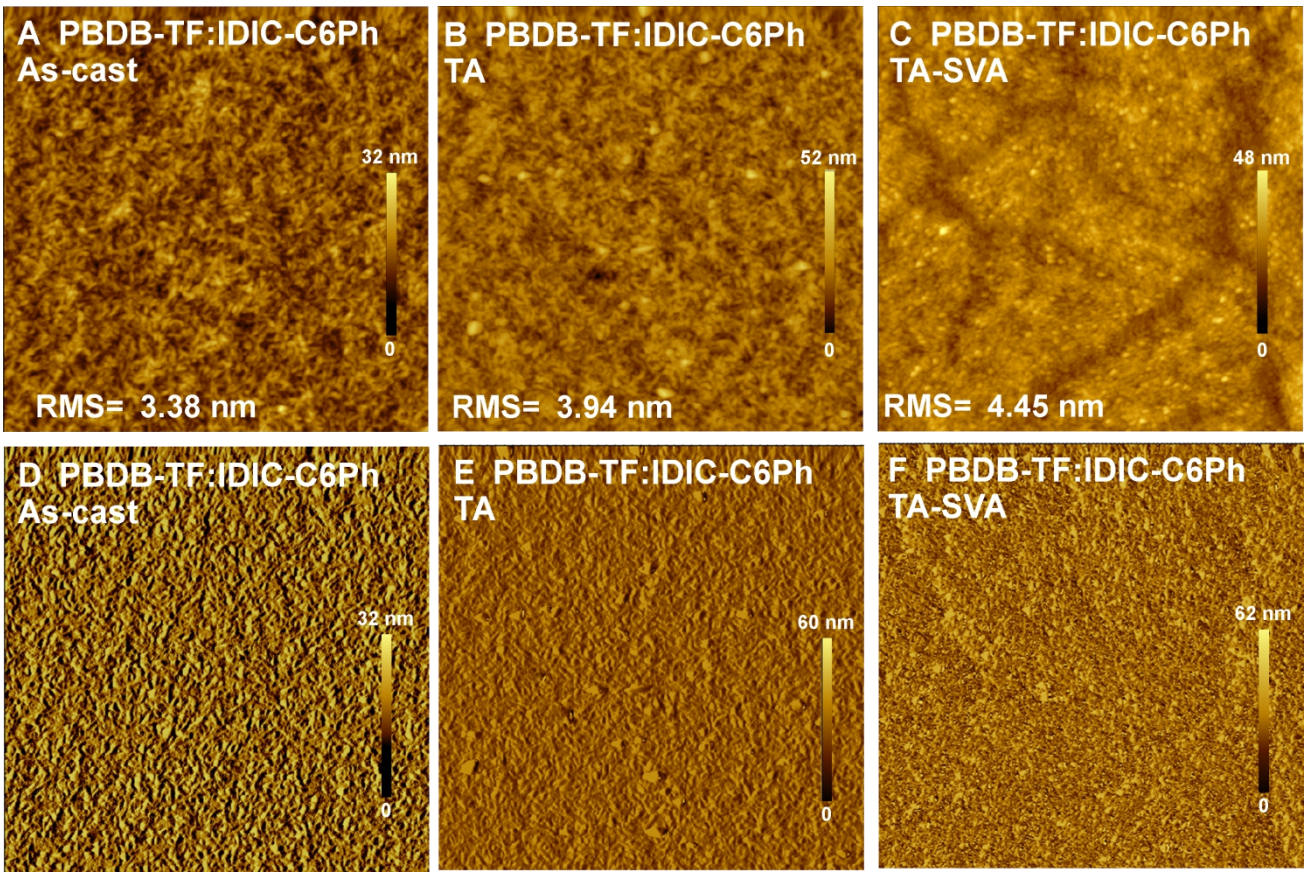

Figure S25. (A-C) The AFM and (D-F) phase images of PBDB-TF:IDIC-C6Ph under different treatments.

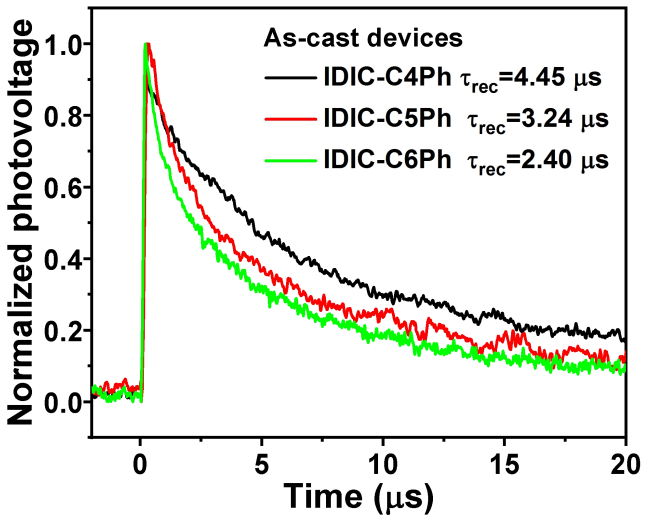

Figure S26. The transient photovoltage (TPV) decay kinetics of three as-cast devices.

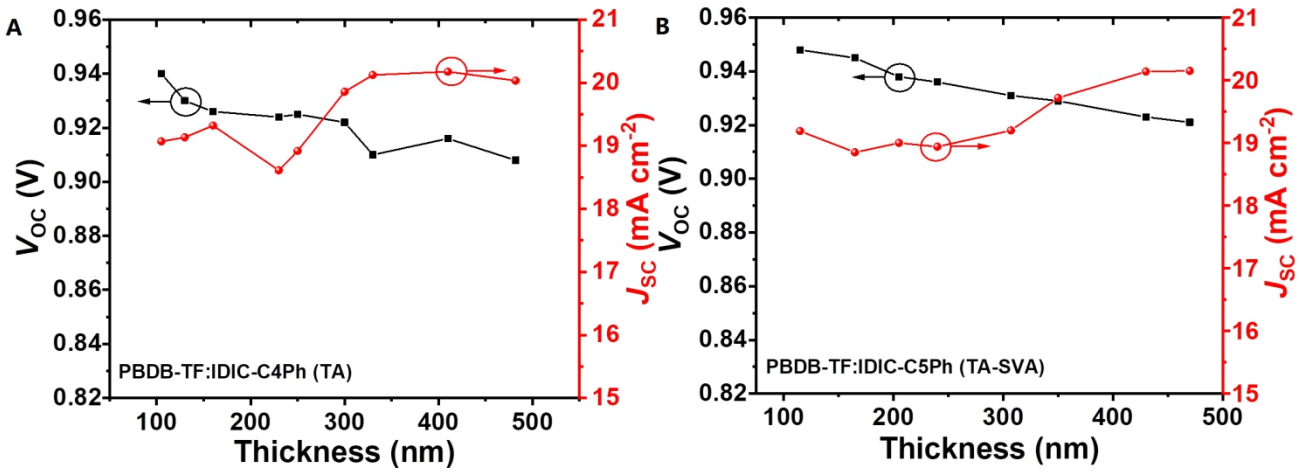

Figure S27. The V_{OC} and J_{SC} of the optimal solar cells (A) PBDB-TF:IDIC-C4Ph and (B) PBDB-TF:IDIC-C5Ph *versus* the active layer film thickness.

Table S6. The photovoltaic performance of PBDB-TF:IDIC-C4Ph (TA) and PBDB-TF:IDIC-C5Ph (TA-SVA) based thick-film OSCs

Blend	Film thickness	V_{OC}	J_{SC}	FF	PCE
	nm	(V)	(mA cm^{-2})	(%)	(%)[a]
PBDB-TF:IDIC-C4Ph	482	0.908	20.03	65.26	11.87
	410	0.916	20.17	68.31	12.62
	330	0.910	19.90	71.35	12.92
	300	0.922	19.85	70.20	12.86
	250	0.925	18.92	74.53	13.02
	230	0.924	18.61	76.49	13.16
	160	0.926	19.32	75.21	13.50
	130	0.930	19.13	78.02	13.88
	105	0.942	18.96	78.05	13.94
PBDB-TF:IDIC-C5Ph	470	0.921	20.15	70.12	13.01
	430	0.923	20.14	72.03	13.39
	350	0.929	19.72	73.75	13.51
	307	0.931	19.20	75.51	13.49
	240	0.936	18.94	78.76	13.96
	205	0.938	19.01	79.02	14.08
	165	0.945	18.85	79.71	14.20
	115	0.948	19.19	80.02	14.56

The film thickness were controlled by changing the total concentration of donor/acceptor (18 mg ml^{-1} to 40 mg ml^{-1}), and the spin-coating speed (500 rpm to 4000 rpm).

Table S7. The photovoltaic performance of thick-film OSCs

	Active layer	Film thickness (nm)	V_{OC} (V)	J_{SC} (mA cm^{-2})	FF (%)	PCE (%)	Ref.
1	PBDB-TF:	300	0.922	19.85	70.20	12.86	This work
2	IDIC-C4Ph	482	0.908	20.03	65.26	11.87	This work
3		**307**	**0.931**	**19.20**	**75.51**	**13.49**	This work
4	PBDB-TF:	350	0.929	19.72	73.75	13.51	This work
5	IDIC-C5Ph	430	0.923	20.14	72.03	13.39	This work
6		**470**	**0.921**	**20.15**	**70.12**	**13.01**	This work
7	PM7:MF1	312	0.934	17.21	74.9	12.03	S1
8		445	0.931	17.06	69.9	11.11	S1
9		308	0.952	19.54	66.1	12.34	S1
10	PM7:MF2	438	0.955	19.35	59.8	11.04	S1
11		500	0.953	19.20	54.9	10.04	S1
12	PBDB-T: IDT-OB	320	0.87	16.34	60.0	8.57	S2
13		420	0.86	17.00	50.2	7.39	S2
14		500	0.84	17.23	47.9	6.93	S2
15	PBDB-TF:IDTN	380	0.91	17.86	58.0	9.40	S3
16		315	0.92	18.11	64.1	10.6	S4
17	PTQ10:IDTPC	400	0.91	17.90	61.3	10.0	S4
18		505	0.91	17.81	56.9	9.2	S4
19	PTQ10:IDIC	310	0.94	19.16	57.1	10.3	S5
20	J61:m-ITIC	360	0.882	19.04	49.36	8.34	S6
21	PBDB-T: m-ITIC-O-EH	302	0.86	15.58	54	7.32	S7
22	PM6:Y6	300	0.823	26.5	62.3	13.6	S8
23	PffBT4T-2OD: PC61BM	300	0.78	17.5	75	10.2	S9
24	PNT4T-2OD: PC71BM	300	0.76	19.8	68	10.1	S9
25	PPDT2FBT: PC71BM	290	0.79	16.3	73	9.39	S10
26	DT-PDPP2T-TT: PC71BM	340	0.67	20.1	70	9.4	S11
27	BTR:PC71BM	330	0.89	12.71	69	7.9	S12
28		400	0.88	12.71	68	7.6	S12

NMR spectra (Figures S27-S40)

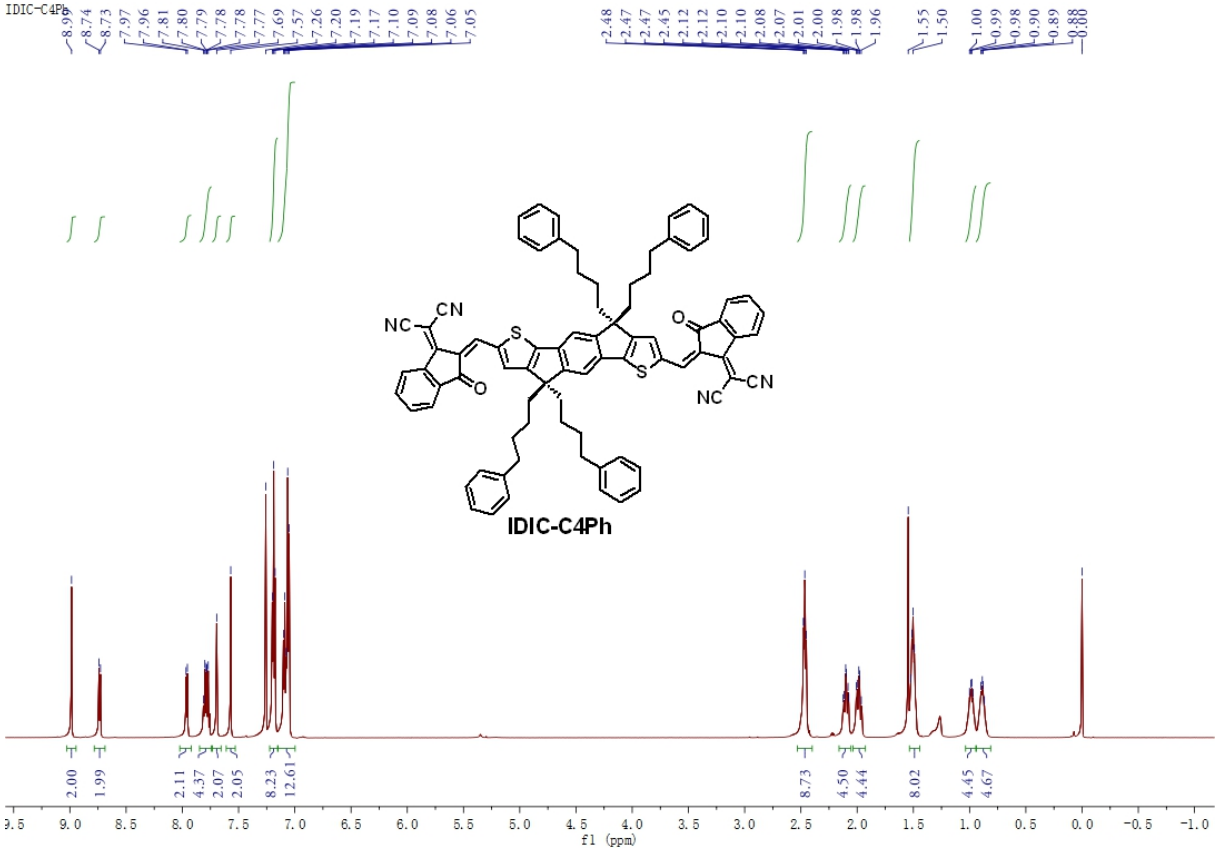

The ^{1}H NMR spectrum of IDIC-C4Ph.

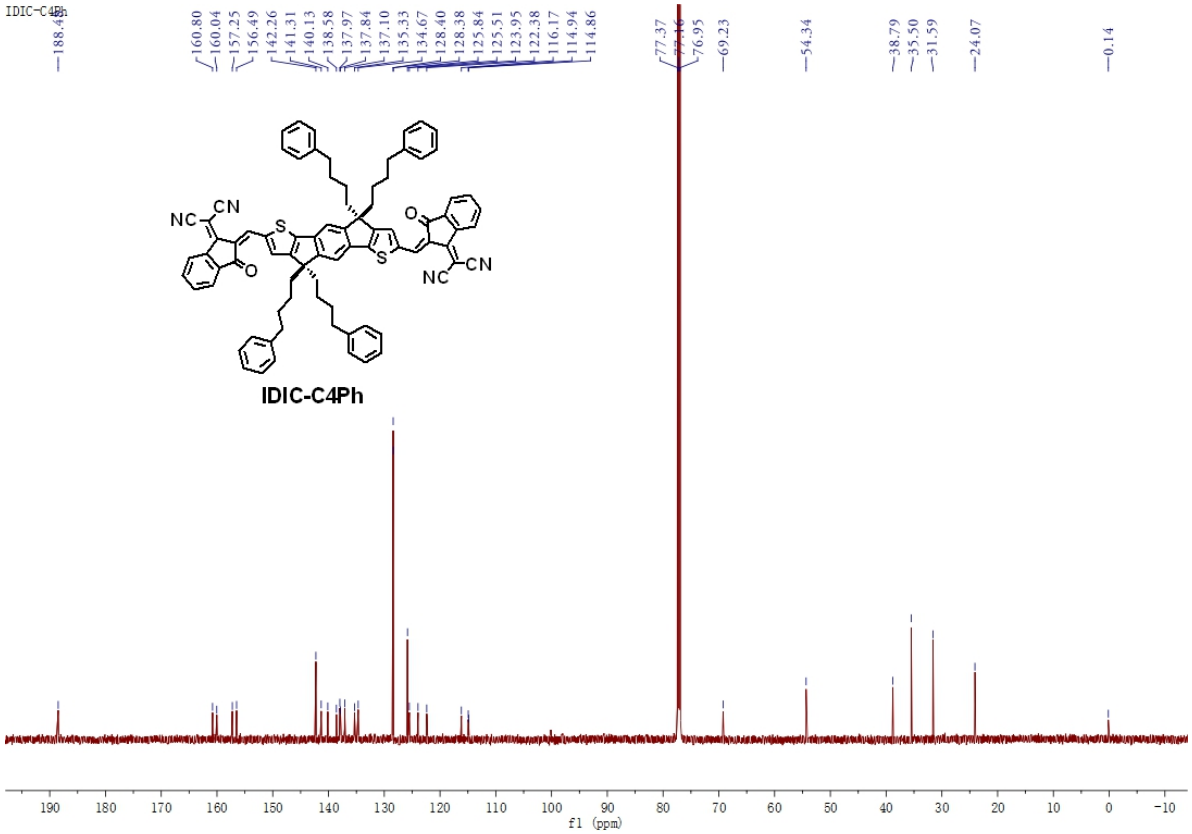

The ^{13}C NMR spectrum of IDIC-C4Ph.

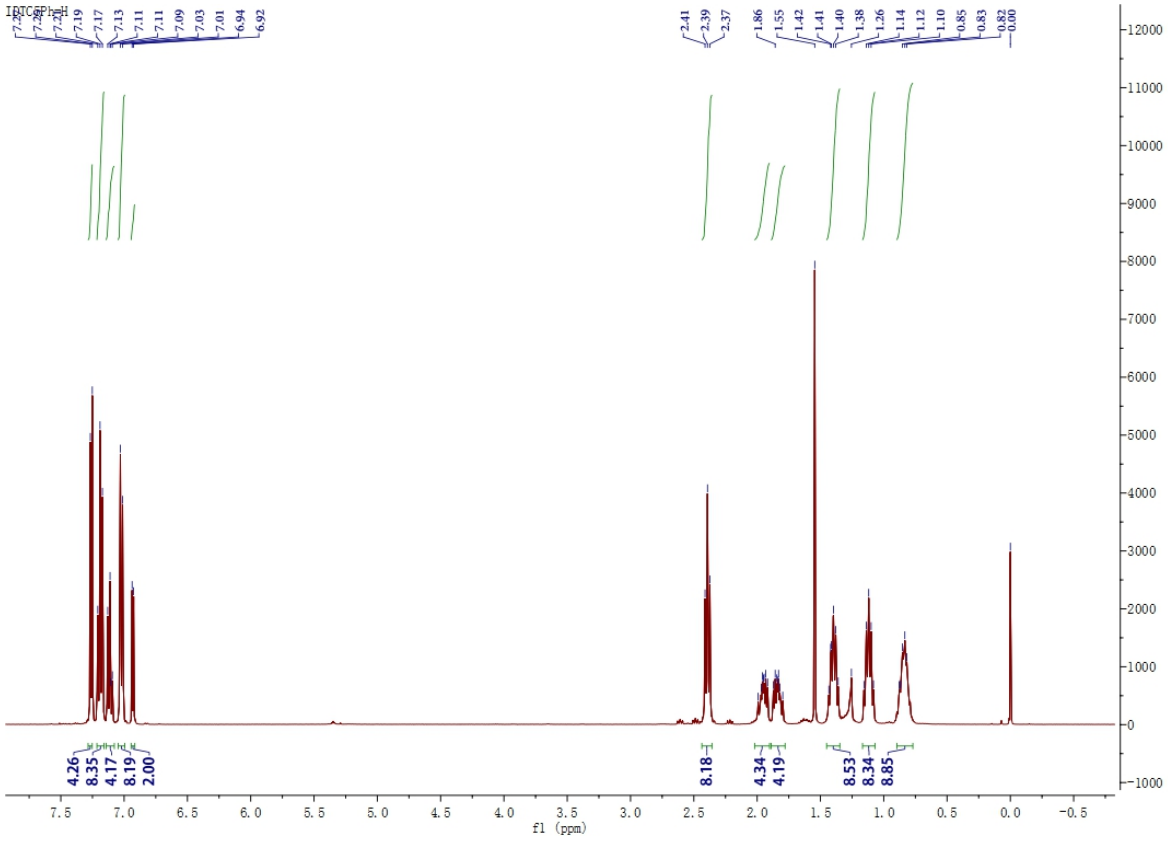

The ^{1}H NMR spectrum of IDTC5Ph.

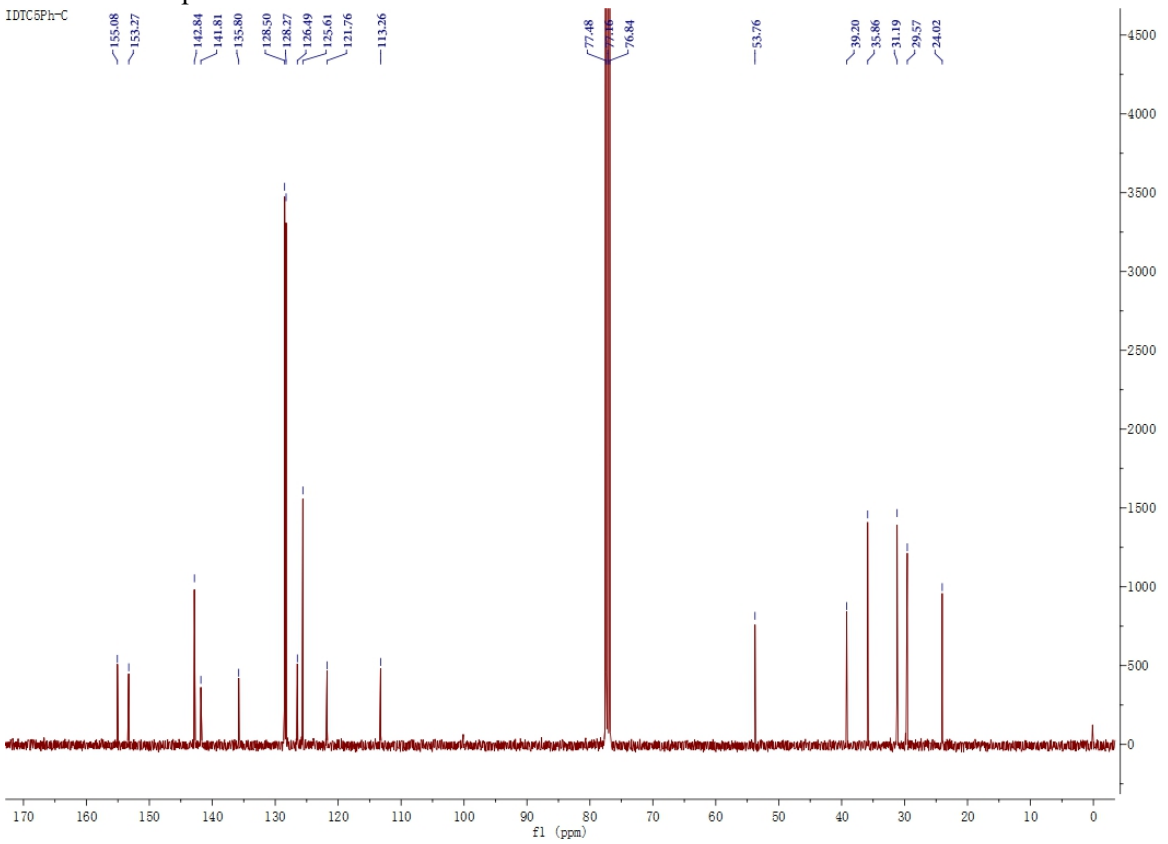

The ^{13}C NMR spectrum of IDTC5Ph.

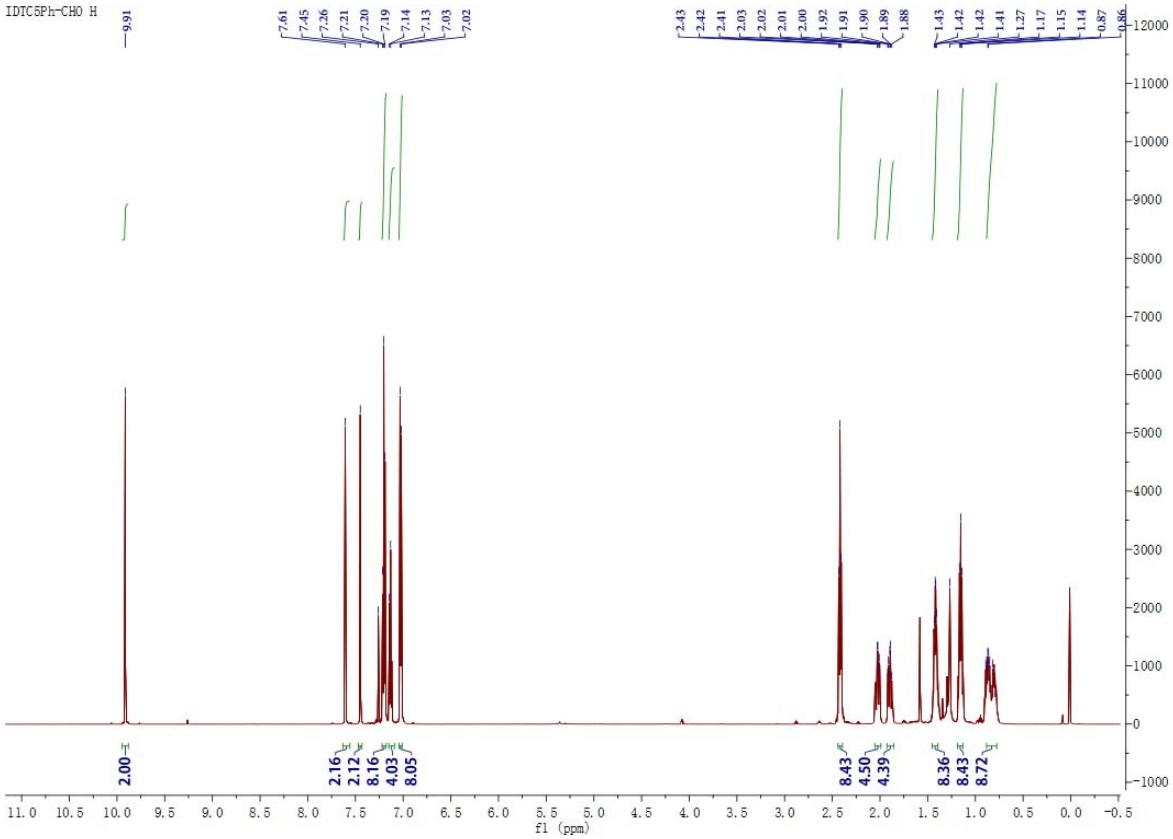

The ^{1}H NMR spectrum of IDTC5Ph-CHO.

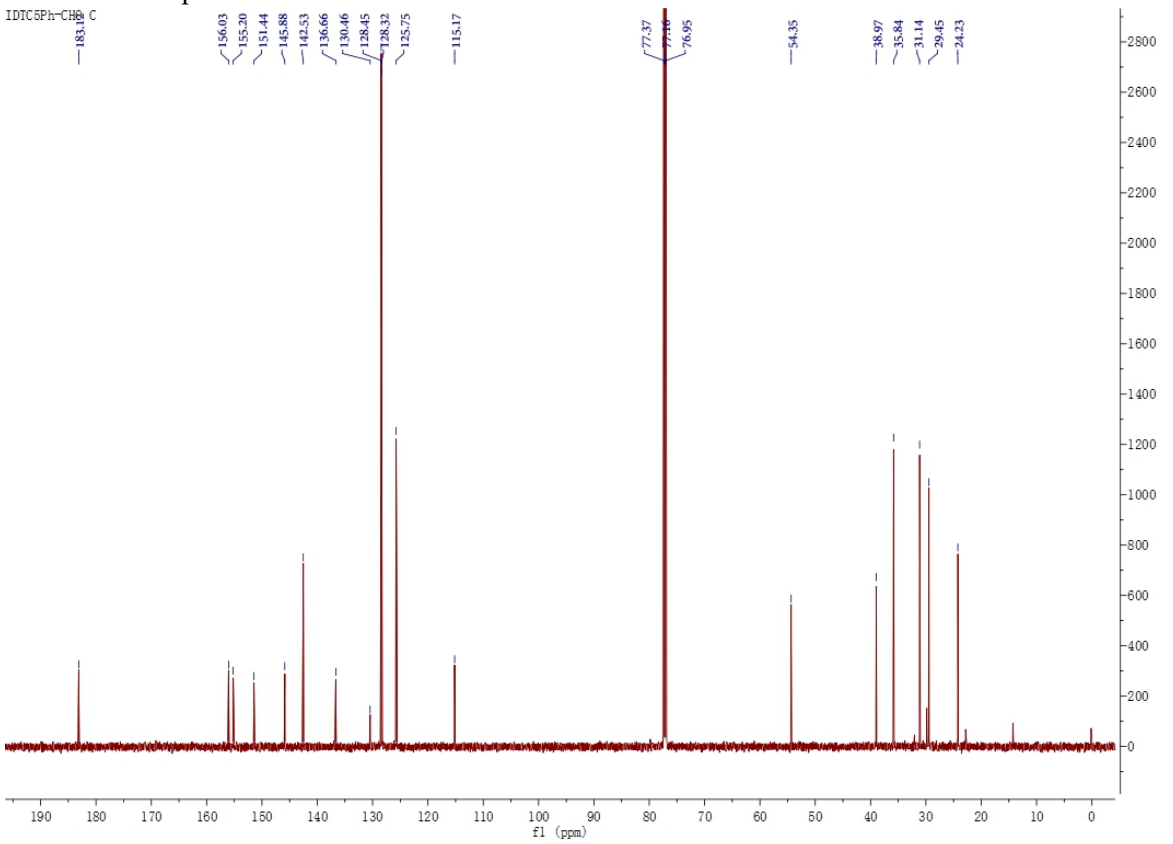

The ^{13}C NMR spectrum of IDTC5Ph-CHO.

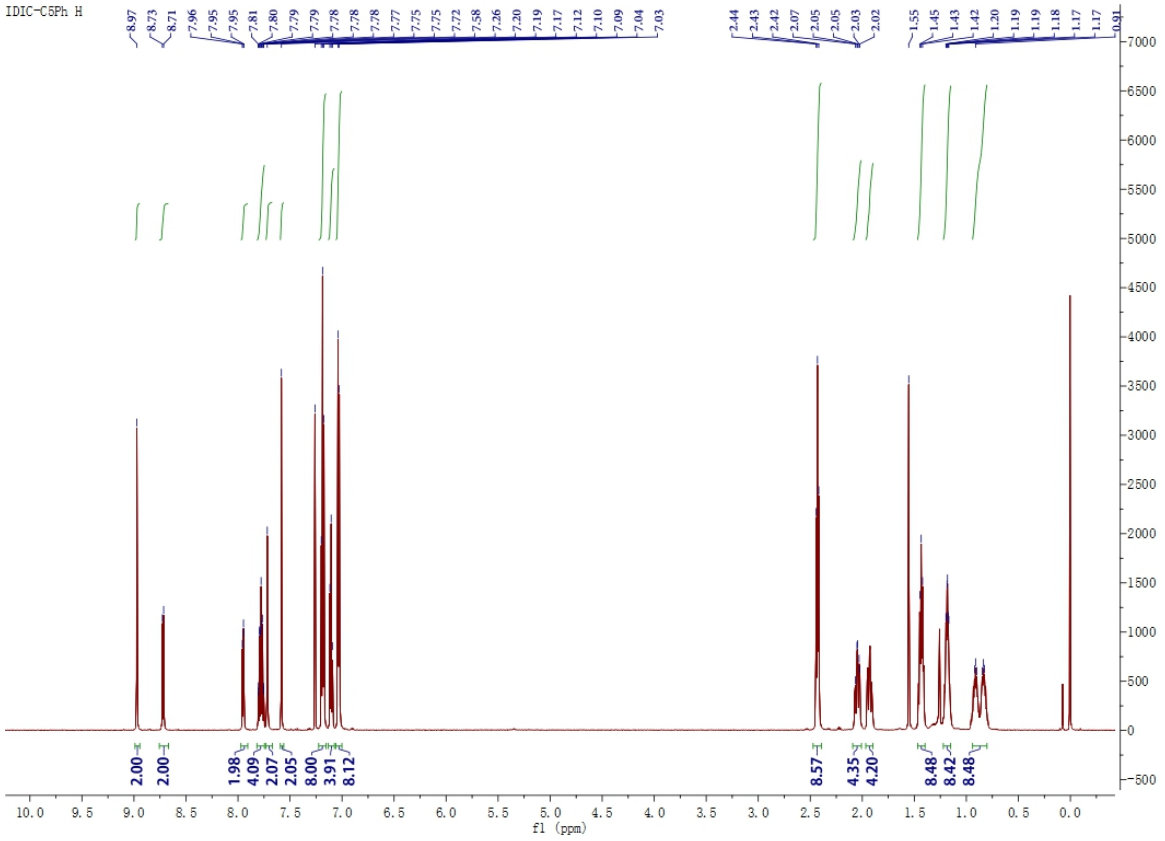

The ^{1}H NMR spectrum of IDIC-C5Ph.

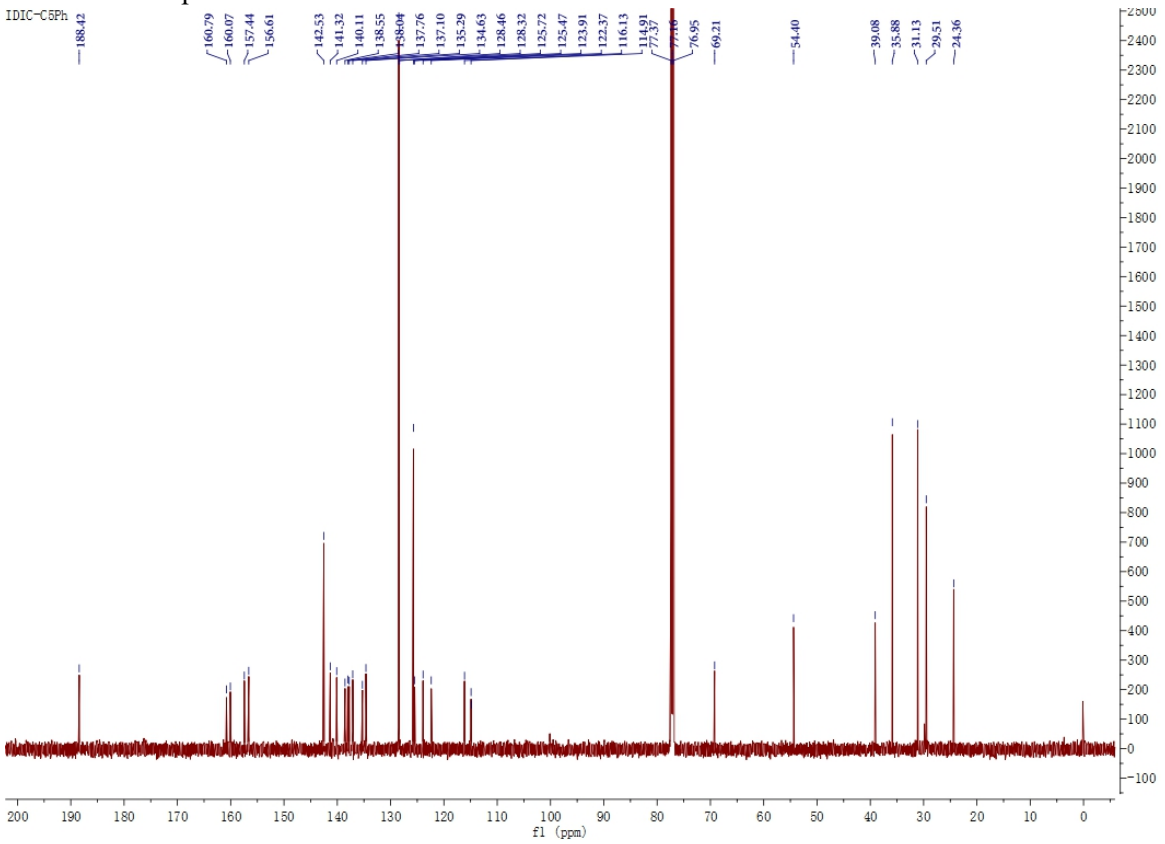

The ^{13}C NMR spectrum of IDIC-C5Ph.

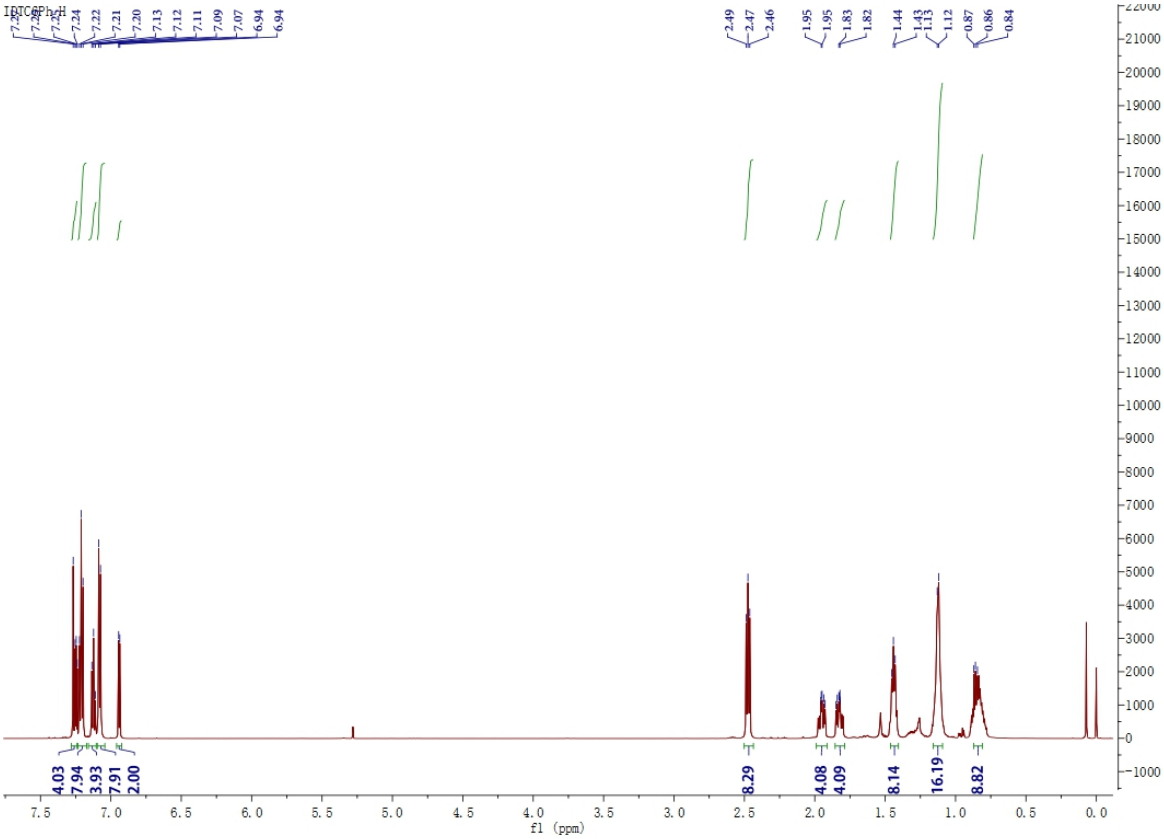

The ^{1}H NMR spectrum of IDTC6Ph.

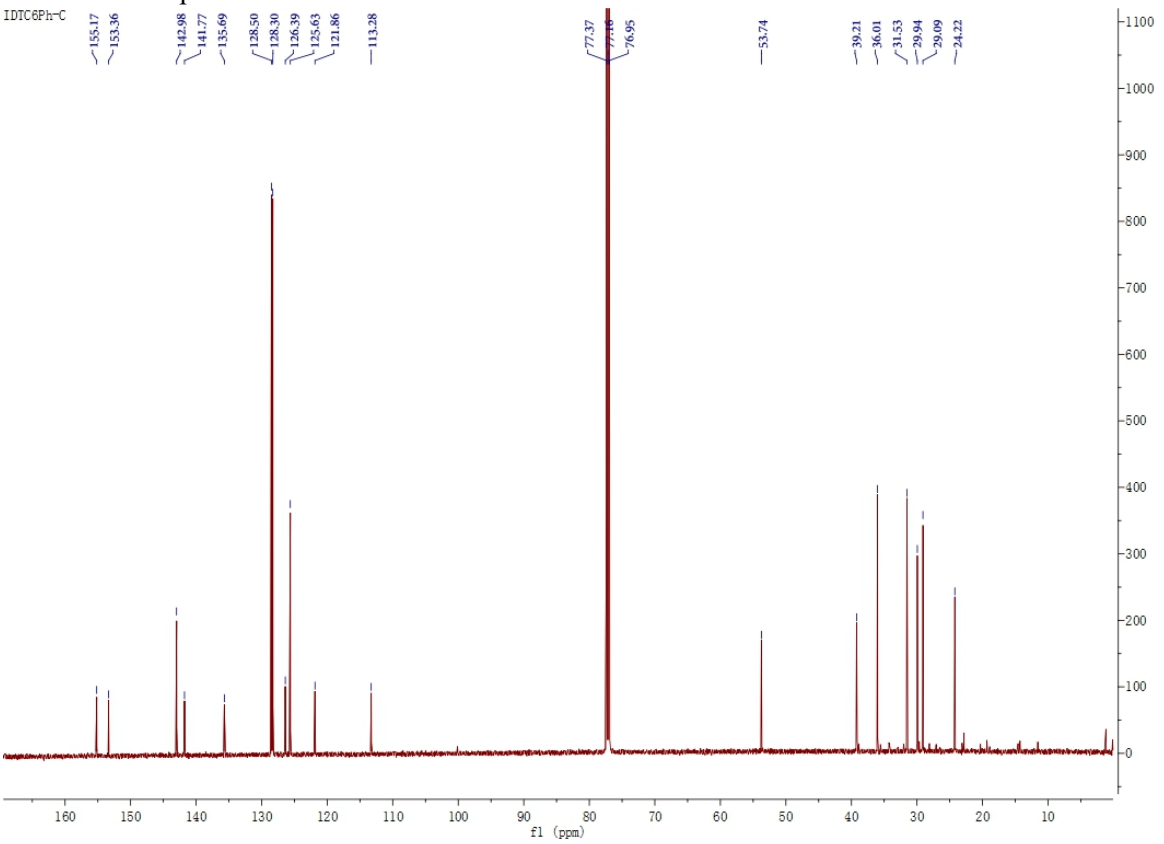

The ^{13}C NMR spectrum of IDTC6Ph.

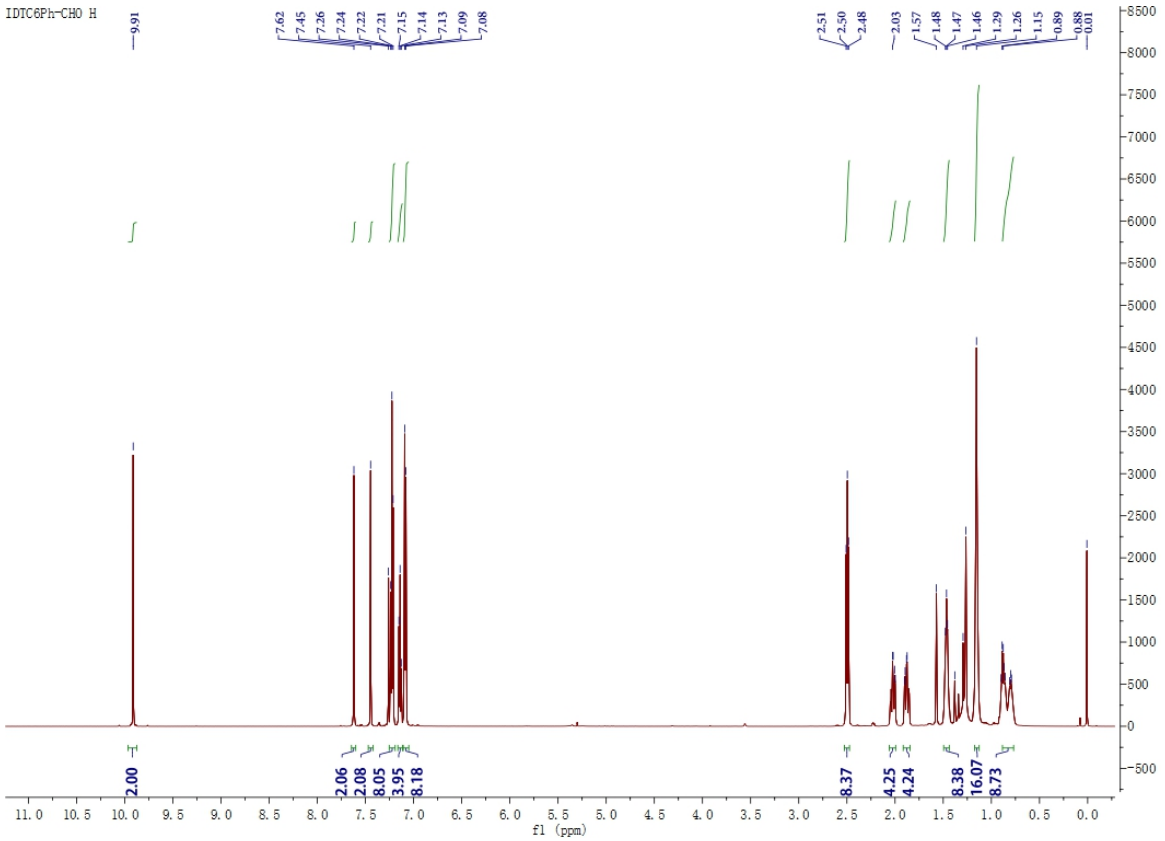

The ^{1}H NMR spectrum of IDTC6Ph-CHO.

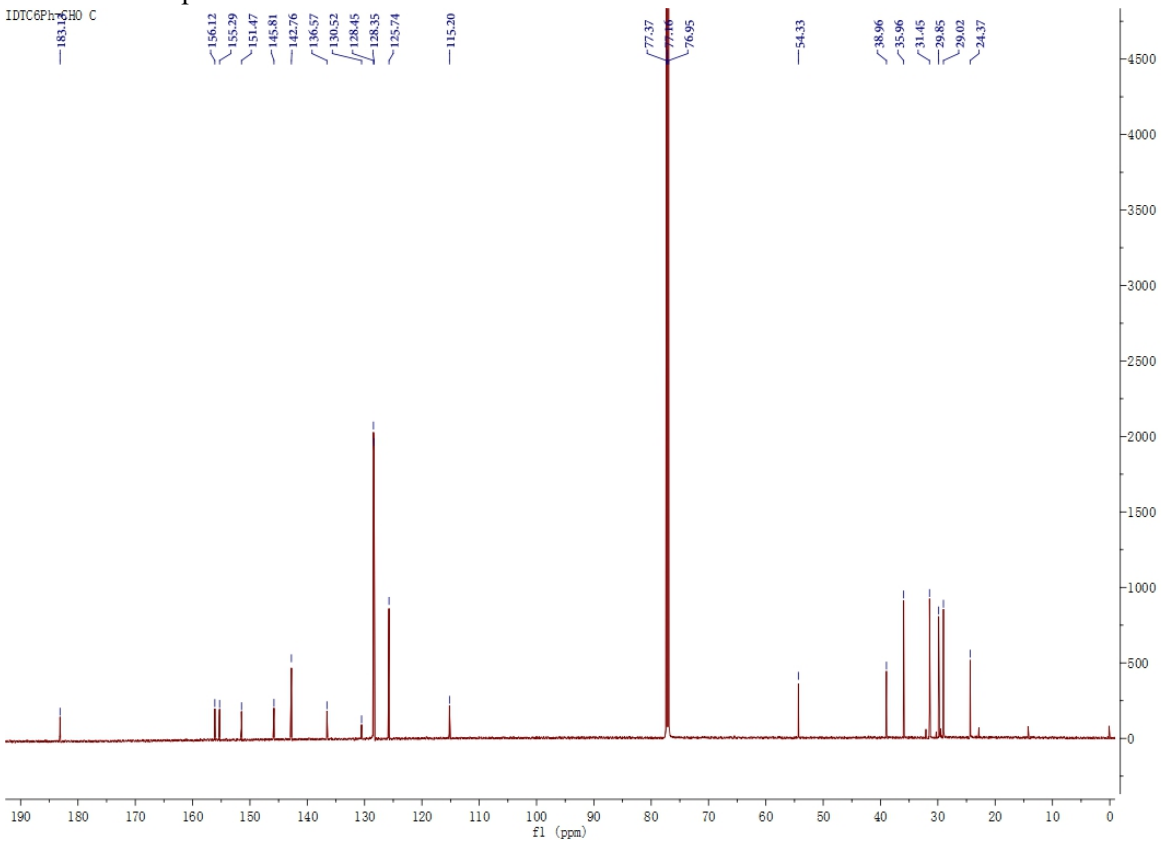

The ^{13}C NMR spectrum of IDTC6Ph-CHO.

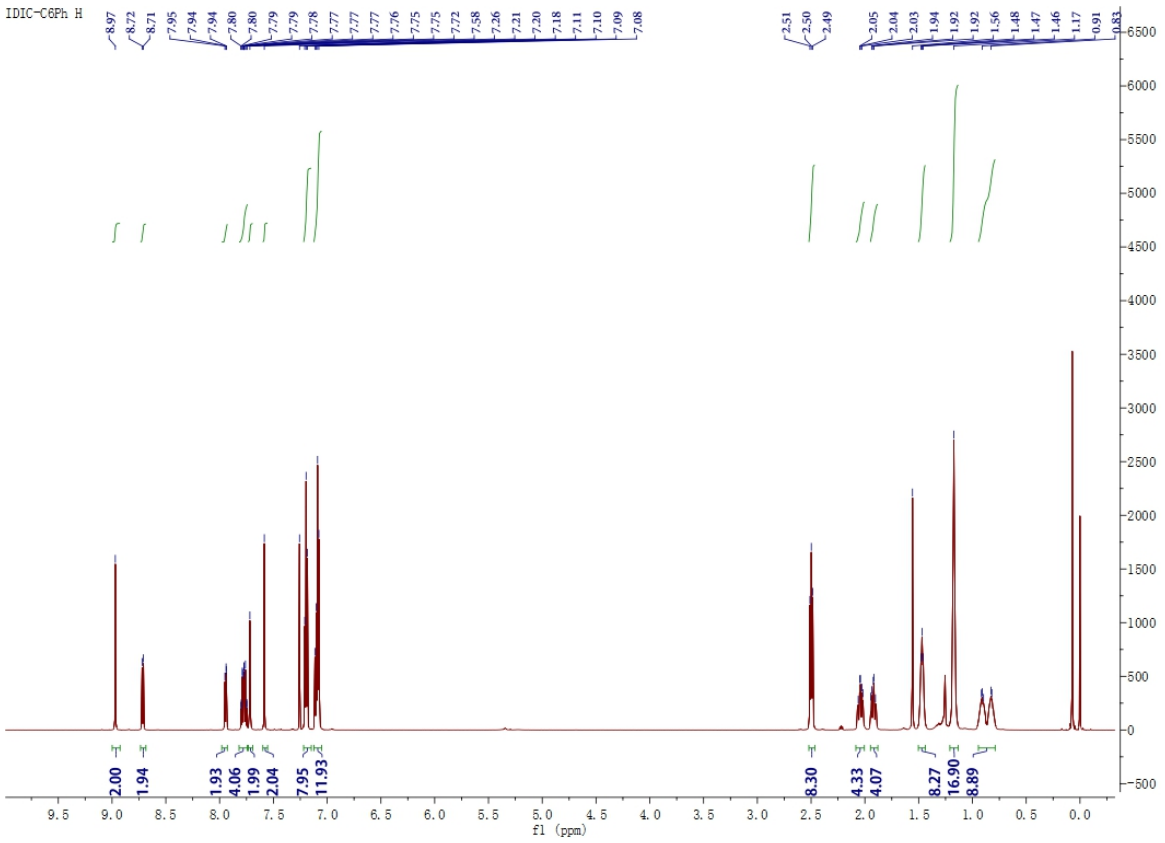

The ^{1}H NMR spectrum of IDIC-C6Ph.

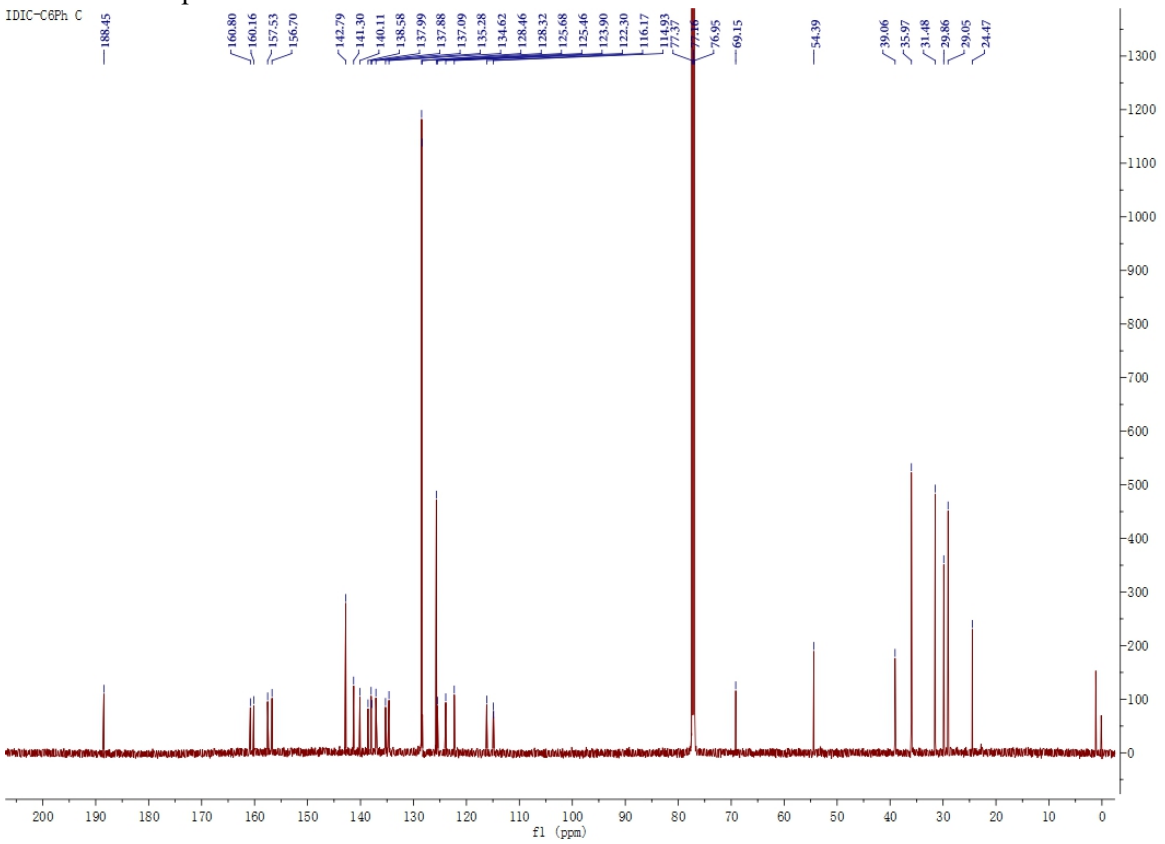

The ^{13}C NMR spectrum of IDIC-C6Ph.

References:

S1 Gao, W., An, Q., Hao, M., et al. (2020). Thick‐film organic solar cells achieving over 11% efficiency

and nearly 70% fill factor at thickness over 400 nm. Adv. Funct. Mater. ***30***, 1908336.

S2 Feng, S., Zhang, C., Liu, Y., et al. (2017). Fused-ring acceptors with asymmetric side chains for high-performance thick-film organic solar cells. Adv. Mater. ***29***. 1703527.

S3 Li, S., Ye, L., Zhao, W., et al. (2017). Design of a new small-molecule electron acceptor enables efficient polymer solar cells with high fill factor. Adv. Mater. ***29***. 1704051.

S4 Sun, C., Pan, F., Bin, H., et al. (2018). A low cost and high performance polymer donor material for polymer solar cells. Nat. Commun. ***9***, 743.

S5 Luo, Z., Sun, C., Chen, S., et al. (2018). Side-chain impact on molecular orientation of organic semiconductor acceptors: high performance nonfullerene polymer solar cells with thick active layer over 400 nm. Adv. Energy Mater. ***8***, 1800856.

S6 Yang, Y., Zhang, Z.G., Bin, H., et al. (2016). Side-chain isomerization on an n-type organic semiconductor itic acceptor makes 11.77% high efficiency polymer solar cells. J. Am. Chem. Soc. ***138***, 15011-15018.

S7 Lee, S., Park, K.H., Lee, J.H., et al. (2019). Achieving thickness‐insensitive morphology of the photoactive layer for printable organic photovoltaic cells via side chain engineering in nonfullerene acceptors. Adv. Energy Mater. ***9***, 1900044.

S8 Yuan, J., Zhang, Y., Zhou, L., et al. (2019). Single-junction organic solar cell with over 15% efficiency using fused-ring acceptor with electron-deficient core. Joule ***3***, 1140-1151.

S9 Liu, Y., Zhao, J., Li, Z., et al. (2014). Aggregation and morphology control enables multiple cases of high-efficiency polymer solar cells. Nat. Commun. ***5***, 5293.

S10 Nguyen, T.L., Choi, H., Ko, S.J., et al. (2014). Semi-crystalline photovoltaic polymers with efficiency exceeding 9% in a ~300 nm thick conventional single-cell device. Energy Environ. Sci. ***7***, 3040-3051..

S11 Choi, H., Ko, S.J., Kim, T., et al. (2015). Small-bandgap polymer solar cells with unprecedented short-circuit current density and high fill factor. Adv. Mater. ***27***, 3318-3324.

S12 Sun, K., Xiao, Z., Lu, S., et al. (2015). A molecular nematic liquid crystalline material for high-performance organic photovoltaics. Nat. Commun. ***6***, 6013.